5-2019

Sequence-Specific Gene Correction of Cystic Fibrosis Airway Basal Cells

Varada Anirudhan

Sequence-Specific Gene Correction of Cystic Fibrosis Airway Basal Cells

by

Varada Anirudhan

Approved:

_____
Brian R. Davis, Ph.D.
Advisory Professor

_____
Burton Dickey, M. D.

_____
Jichao Chen, Ph.D

_____
Sheng Zhang, Ph.D

_____
Philip Ng, Ph.D

Approved:

_____
Dean, The University of Texas
MD Anderson Cancer Center UTHealth Graduate School of Biomedical Sciences

SEQUENCE-SPECIFIC GENE CORRECTION *of*

CYSTIC FIBROSIS AIRWAY BASAL CELLS

A

THESIS

Presented to the Faculty of

The University of Texas

MD Anderson Cancer Center

UTHealth Graduate School of Biomedical Sciences

in Partial Fulfillment of the Requirements

of the Degree of

MASTER OF SCIENCE

By

Varada Anirudhan, B. Tech.

Houston, Texas

May 2019

Dedicated to my mom, dad, and sister

Acknowledgments

I would like to express my gratitude towards my supervisor, Dr. Brian Davis, for his constant support throughout the period of my master's course. His achievements, hard work and humility truly inspire me; he has patiently guided me, challenging me and providing me the necessary criticism when required, which in turn has helped me develop into a much better scientist than I was before I joined his lab.

I would also like to thank the current and former members of my lab for all the guidance they have provided me during my time here and for making the lab a wonderful place for me to learn while also having fun doing some interesting research: Drs. Ana Crane, Shingo Suzuki (who has taught me a number of technical skills, for which I will forever be thankful), Nadine Matthias, John Avila, Cristina Barillá, and Leila Rouhigharabaei. I am grateful to our collaborators, Drs. Eric Sorscher and Andras Rab for their immense help in performing Ussing chamber studies for my project. I would like to thank also Dr. Anthony Conway, our collaborator at Sangamo Therapeutics, for performing, as part of my project, Next-Generation Sequencing analysis. Thank you Dr. Zhengmei Mao for your help with the histology studies for my project.

I would like to thank my advisory committee members Drs. Burton Dickey, Philip Ng, Jichao Chen and Sheng Zhang for their constant supervision throughout my project work. Along with Dr. Davis, each of them have been involved in improving my thinking abilities as a researcher.

Thank you GSBS, first of all, for accepting me into your MS program, and everyone at the GSBS office (especially Drs. Eric Swindell and Lindsey Minter), I am grateful to you for being so kind towards me, helping me when needed and answering so patiently

even my silliest questions.

Words cannot express how thankful I am to my mother, father and sister for their unconditional love and faith in me. I owe them so much; this degree is more theirs than it is mine. My closest friends here in Houston, Kaavya and Henry, thank you for having my back. Last but certainly not the least, Saravanan, my pillar of strength, thank you for always being there.

Sequence-Specific Gene Correction of Cystic Fibrosis Airway Basal Cells

Varada Anirudhan, B. Tech.

Advisory Professor: Brian Davis, PhD

Cystic fibrosis (CF) is a lethal monogenic disease resulting from mutations in the *CFTR* gene which encodes a protein involved in regulating anion trans-epithelial transport. A three-base deletion in *CFTR* (termed as ΔF508 mutation), wherein CFTR protein is misfolded leading to its pre-mature degradation in the endoplasmic reticulum (ER), is the most common cause of this debilitating disease. Since CFTR is expressed in multiple body systems, CF affects different organs, but lung pathology is the greatest cause of death in affected patients. We achieved site-specific gene correction with an efficiency of ~10 % in CF airway basal cells homozygous for the ΔF508 mutation. Basal cells are a multipotent stem cell population of the respiratory epithelium and therefore, their gene correction could provide a long-term, permanent remedy for CF. Delivery of engineered sequence-specific zinc finger nucleases (ZFNs) and single-stranded oligo DNA (ssODN) carrying the correcting sequence via electroporation facilitated the correction. The gene-corrected cells upon *in vitro* differentiation using air-liquid interface showed presence of fully-glycosylated mature CFTR protein as opposed to differentiated mutant cells which synthesized only the core-glycosylated immature form. Most importantly, we demonstrated CFTR ion channel activity in the gene-corrected cells by Ussing chamber electrophysiology.

TABLE OF CONTENTS

LIST OF TABLES

LIST OF FIGURES

ABBREVIATIONS

56BP1	Tumor suppressor p53-binding protein 1
AAV	Adeno-associated virus
ACT	Acetylated-tubulin
APC	Allophycocyanin
ALI	Air-liquid interface
AS-PCR	Allele-specific PCR
B2M	Beta-2-microglobulin
BCA	Bicinchoninic acid
BMP	Bone morphogenetic protein
BrdU	Bromodeoxyuridine / 5-bromo-2'-deoxyuridine
BSA	Bovine serum albumin
CCR5	C-C chemokine receptor type 5
cDNA	complementary DNA
CD49f	Cluster of differentiation 49f
CD271	Cluster of differentiation 271
CF	Cystic fibrosis
CFTR	Cystic fibrosis transmembrane conductance regulator

CK5	Cytokeratin 5
CK14	Cytokeratin 14
CRC	Conditionally-reprogrammed culture
CRISPR	clustered regularly interspaced short palindromic repeats
DAPI	4,6’-diamidino -2-phenylindole
DSB	Double-stranded DNA break
ER	Endoplasmic reticulum
FOXI1	Forkhead box I1
FOXJ1	Forkhead box J1
gDNA	Genomic DNA
GAPDH	Glyceraldehyde 3-phosphate dehydrogenase
H&E	Hematoxylin and eosin
HSC	Hematopoietic stem cell
HDR	Homology-directed repair
iPSC	Induced pluripotent stem cell
INDEL	insertions and deletions
kDa	Kilo Dalton
mRNA	messenger RNA

MUC5AC	Mucin 5AC
NGFR	Nerve growth factor receptor
NHEJ	Non-homologous end joining
NS	Non-significant
p63	Transformation-related protein 63
PCR	Polymerase chain reaction
PE	Phycoerythrin
P-ex plus	Pneumacult-Ex plus
RIPA	Radioimmunoprecipitation assay
ROCK	Rho-associated protein kinase
RT-PCR	Reverse transcription PCR
ssODN	Single-stranded oligo DNA
SCID	Severe combined immune-deficiency
SD	Standard deviation
SO_2	Sulphur dioxide
TALEN	Transcription activator-like effector nucleases
TGF-β	Transforming growth factor-β
TIDER	Tracking of Insertions Deletions and Recombination Events

WT	Wild-type
ZFN	Zinc finger nuclease
ZFN-L	Zinc finger nuclease-left component
ZFN-R	Zinc finger nuclease-right component

CHAPTER 1: INTRODUCTION

1.1 Cystic Fibrosis (CF)

A lethal recessive autosomal disease, cystic fibrosis (CF) is common in populations of northern European descent with an incidence rate of about 1 in 2000 births (*2*). Mutations in the gene that encodes the cystic fibrosis transmembrane regulator (CFTR) protein results in CF. Less than 200 mutations among the ~2000 that have been identified in the *CFTR* gene have been demonstrated to result in CF (*2*). Based on their impact at the cellular level, the *CFTR* mutations fall into six distinct classes (TABLE 1.1). The most common *CFTR* mutation (ΔF508), comprising 66% of all mutations, belongs to class II and causes the deletion of phenylalanine at position 508 of CFTR. The ΔF508 CFTR protein is improperly folded leading to its retention in the endoplasmic reticulum (ER) and eventual degradation by the proteasome in a ubiquitin-dependent fashion which drastically reduces protein delivered to the cell surface (*7*). CFTR channel opening is also defective in ΔF508 CF patients (*15*). The *CFTR* gene is located on chromosome 7, has 27 exons and the three-base-pair ΔF508 deletion occurs in exon 11.

1.1.1 CF Pathophysiology

CFTR functions as an anion channel primarily for chloride and bicarbonate transport. In CF patients, the epithelial cells are characterized by decreased chloride secretion and increased sodium absorption (*4*). Although CF affects multiple organs including the lungs, pancreas, liver, intestine, bones and male reproductive tract (*2*), the pulmonary manifestations are the major cause for CF morbidity and mortality (*3*). This is because the regulatory role of CFTR to balance salt and fluid transport is disrupted leading to thick and sticky mucus being produced along the airway which paves the way for micro-

organisms to invade and infect the lung (*14*). CF lung infection is mainly caused by *Staphylococcus aureus*, *Hemophilus influenza*, and *Pseudomonas aeruginosa* (*4*). Other CF symptoms include maldigestion, and fat & protein malabsorption resulting from pancreatic insufficiency (occurring in 90% of CF patients) (*5*), gastroesophageal reflux (*4*) and symptomatic cholelithiasis (occurring in ~5% of CF patients) (*6*).

1.1.2 CF Treatment

The median survival when CF was first described in 1938 (*8*) was less than 1 year of age and now it is 46.2 years in the United States (*9*) and 41 in the UK (*2*) owing to early detection and improved treatment methods. Frequent prolonged courses of antibiotic treatment help improve pulmonary function (*10*). Viral infection in the respiratory tract can be prevented with the help of vaccination against measles, chicken pox and influenza. Standard chest physical therapy, mechanical vests and directed exhalation techniques aid in controlling airway obstruction (*4*). Treatment using aerosolized 7% hypertonic saline solution has shown clinically-relevant benefits in ameliorating CF symptoms (*93, 94*).

CFTR modulators are therapeutic small molecules that have proved beneficial to a growing number of CF patients (*11, 12, 13*) and include “CFTR potentiators” which increase epithelial CFTR activity & “CFTR correctors” that improve defective protein misfolding and trafficking. The primary target of the CFTR potentiator Kalydeco® (ivacaftor, IVA; Vertex Pharmaceuticals, Boston, MA, USA) is a Class III CFTR mutation known as G551D in which CFTR channel has a lower open probability than wild-type CFTR. Orkambi® (Vertex Pharmaceuticals, Boston, MA, USA), an agent containing two compounds including lumacaftor and IVA (also known as VX809 and VX770), increases

CFTR protein deposition on cell surfaces by acting as molecular chaperones during protein folding and has shown promising results in treating ΔF508 CF. Currently, in late-stage clinical trials are three-drug combination (VX-659 + tezacaftor + ivacaftor) potentially capable of treating up to 93% of CF patients, including those with the ΔF508 mutation in at least one allele (*88*).The CFTR modulators, however, are expensive, and require lifetime treatment (*16*).

TABLE 1.1 The six classes of *CFTR* mutations and their respective phenotypic defects:

Class	Defect	Example
I	defective protein production	Gly542X
II	defective protein processing	ΔF508
III	defective channel regulation	G551D
IV	defective conduction	Arg117His
V	reduction in functional CFTR protein	2789 + 5G
VI	decreased CFTR stability	4326delTC

1.2 Airway Basal Cells (BCs)

The lung originates from the foregut endoderm and has two major regions: the airways which conduct gases and the alveoli where gas exchange occurs. Although it includes mesenchymal, endothelial and neural compartments, the epithelial cell lineages of the lung have been best-characterized. Most of these studies have been conducted, however, in the murine lung and therefore it is important to note that the human lung may have additional unique properties that are yet to be studied.

In the proximal lung region, the upper airways and bronchi (comprising large airway region) contain superficial epithelium and submucosal glands. Small or distal airways (bronchioles) contain only superficial epithelium. The lung epithelium in large airways is pseudostratified and is composed mainly of basal (BC), secretory, and ciliated cells (*37*) and rare neuroendocrine cells (*51*). Cytokeratin 5 (CK5) and 14 (CK14) preferentially expressed in the basal cells help them firmly attach to the basement membrane via hemidesmosomes (*38*). This property contributes to the structural role of basal cells wherein they help tether the columnar epithelial cells to the airway wall (*47*). They also characteristically express the transcription factor Tp63 (p63) (*45*) and nerve growth factor receptor (NGFR) (*39*). Boers *et al.* (1998) (*37*) showed that the distribution of airway basal cells varies along the length of the airways with ~31% basal cells in the largest conducting airways (diameter ≥ 4 mm) and 6% in the smallest airways (diameter < 0.5 mm). Based on several studies (*39, 40, 41, 42*), there is now evidence that the airway BCs are a multipotent stem cell population. Firstly, Randell *et al.* (2000) (*43*) suggested the existence of stem-cell niches in the pseudostratified epithelium of mouse trachea based on BrdU (bromodeoxyuridine/5-bromo-2'deoxyuridine) label retention over long term after epithelial cell damage by SO_2 inhalation. Hong and colleagues (2003) (*44*) demonstrated that CK14-expressing basal cells proliferate and re-establish the normal epithelium *in vivo* following naphthalene-induced secretory cell depletion. Hajj *et al.* (2007), using an *in vivo* humanized nude mouse xenograft model and an *in vitro* air-liquid interface culture model, demonstrated the ability of human airway basal cells to restore a well-differentiated and functional airway epithelium. Similar studies were conducted by Peault B. *et al* (2005) (*48*) as well. Later in 2009, Rock *et al.* (*39*),

through lineage-tracing studies in mouse trachea, demonstrated the ability of basal cells in steady state to self-renew and differentiate to secretory and ciliated cells. With the help of a novel 3-dimensional sphere forming assay, they were able to demonstrate that BCs of both mouse trachea and human airways are a multipotent stem cell population.

Airway basal cells can be expanded *in vitro* using a technique involving co-culture with irradiated 3T3-J2 feeder cells along with a Rho-associated protein kinase (ROCK) inhibitor Y-27362 (*49, 50*). These cells were demonstrated to maintain their tissue-specific stem cell features in that they proliferated and differentiated to secretory and ciliated cells. Mou *et al.* assessed the roles of transforming growth factor-β (TGF-β) and bone morphogenetic protein (BMP) signaling in epithelia and demonstrated that inhibition of these signaling pathways along with a ROCK inhibitor (termed 'dual SMAD inhibition' media) aided in the long-term expansion of airway basal cells (*1*).

1.3 CFTR Expression in the Airway Epithelia

Although CFTR plays a vital role in maintaining normal physiology of lung epithelial cells, it is expressed at very low levels (1-2 CFTR mRNA transcript copies per cell) (*52*). This, along with the low specificity of CFTR antibodies are probably the reasons why studies to elucidate cellular localization of CFTR have shown contradictions. Engelhardt *et al.* (1992) (*54*), using *in situ* hybridization and immunofluorescence studies demonstrated that in the human bronchus the predominant site of CFTR expression was the submucosal glands and rare (1-3% of total cell number) "flask-like" cells present in the submucosal gland ducts. In another study (1994) (*53*), similar observations were reported; in addition, they showed that CFTR expression was undetectable in the ciliated cells although they are believed to be involved in trans-

epithelial ion transport. Kreda and colleagues (*55*) detected CFTR mRNA throughout the lung superficial epithelium and found that the expression level decreased distally. Using immunostaining and high-resolution laser confocal microscopy techniques they showed that CFTR was localized to the apical region of the ciliated cells. They also observed rare cells that were intensely stained by CFTR antibodies.

Most recently, two groups (*51, 56*) identified a new rare lung epithelial cell population which highly expresses CFTR. These cells, named as pulmonary ionocytes, specifically expressed FOXI1 transcription factor and CFTR, comprise <1% of total lung epithelial cells and expressed 54.4% of all detected CFTR mRNA. These results were based on single-cell RNA sequencing analysis on mouse tracheal epithelial cells and *in vitro*-differentiated primary human bronchus epithelial cells (HBECs). However, there is currently no consensus regarding the relative roles for ionocytes versus ciliated cells in functional CFTR activity in the airways.

1.4 Programmable Nuclease-mediated Gene Therapy

The inherent response of a cell to double-stranded DNA breaks (DSBs) is to follow either of the two endogenous DNA repair pathways: non-homologous end-joining (NHEJ) and homology-directed repair (HDR) (*22*). The error-prone NHEJ mechanism results in the creation of insertions and/or deletions of nucleotides (known as INDELs) which can result in a gene ‘knock-out”. In the presence of a donor DNA, the cell can follow the HDR pathway to ‘edit’ or ‘correct’ the genome in the desired way.

Zinc finger nucleases (ZFNs), transcription activator-like effector nucleases (TALENs), and Clustered regularly interspaced short palindromic repeats (CRISPR/Cas9) are three

nuclease systems that have proved their potential to enable genome editing (*23*). Each of these programmable nucleases results in induction of sequence-specific double-stranded DNA breaks (DSBs). This forms the basis for nuclease-mediated gene therapy.

1.4.1 ZFN-mediated Gene Therapy

ZFNs are targetable DNA cleavage reagents that are fusions of a DNA-binding domain and a non-specific FokI endonuclease cleavage domain (FIGURE 1.1). The DNA-binding domain includes zinc finger (ZF) motifs which are engineered to specifically bind to the target sequence of interest and their DNA recognition ability is context-dependent.

The ZFN monomers (ZFN-L and ZFN-R) are inactive by themselves and it is required that two ZFN monomers bind to their adjacent DNA sites and the FokI nuclease domains to dimerize for the ZFN to cause double-stranded DNA breaks (*33*). This property served as an advantage to improve ZFN specificity to avoid off-target cleavage and three research groups (*34, 35, 36*) re-designed the FokI domains (making them obligate heterodimers) permitting cleavage only by ZFN-L/ZFN-R (and not ZFN-L/ZFN-L or ZFN-R/ZFN-R) by which they were able to considerably reduce cytotoxicity resulting from promiscuous cutting by the ZFNs.

Sequence-specific gene targeting can be achieved using ZFNs and has been shown by several studies including that of Porteus (2005) (*27*) where one site each in β-globin and the interleukin-2 receptor common gamma chain (IL-2Rγ) were targeted. Later, the Sangamo Biosciences group designed ZFN pairs that mediated targeting of the hamster dihydrofolate reductase (*DHFR*) gene (*28*) and the human chemokine receptor *CCR*5

gene (*29*). These are examples of gene inactivation where the cell's NHEJ machinery resulted in gene knock-out.

As noted earlier, to add nucleotide sequences, or to 'correct a gene sequence' requires the introduction of a donor DNA carrying the correcting sequence along with the DSB-inducing nuclease such as ZFNs. Urnov *et al.* (2005) (*31*) had achieved an 18% gene correction of an X-linked severe combined immunodeficiency (SCID) mutation in the IL-2Rγ gene using site-specific ZFNs. Moehle *et al.* (2007) (*30*) achieved 5-15% targeted integration in the exon 5 region of the human IL-2Rγ gene using site-specific ZFNs and donor DNA. Both of these studies reported selection-free gene modification and used double-stranded DNA as donors. Chen *et al.* (2011) reported evidence for efficient genome editing using ZFNs and single-stranded DNA oligos (ssODN) where the efficiency of insertion was in the range 7% to 57% and showed that these values were cell-type dependent (32).

1.4.2 Gene Therapy in Stem Cells

Stem cells possess self-renewal and multi-lineage differentiation potential which makes them suitable for regenerative medicine. Several groups have reported successful *ex vivo* viral-based gene delivery (with random integration of therapeutic transgenes) in hematopoietic stem cells (HSCs) from patients with genetic diseases such as Wiskott-Aldrich syndrome (*17, 18*), X-linked severe combined immunodeficiency (SCID) (*19*) and β-thalassemia (*20*). Efficient gene editing to ablate two clinically relevant genes *CCR5* and *B2M* was achieved in HSCs using a CRISPR/Cas9 nuclease system (*21*).

FIGURE 1.1 Action of Zinc Finger Nucleases: *Shown here is a pair of ZFN monomers that result in DSBs upon binding of their DNA-binding domain (orange) to the respective DNA sequences and dimerization of the FokI-endonuclease domains (yellow). In the presence of a donor DNA, the cell's DNA repair pathway can follow homology-directed repair facilitating targeted gene replacement (green), otherwise non-homologous end joining pathway would be followed resulting in insertions (blue) and deletions (red) (INDELs).*

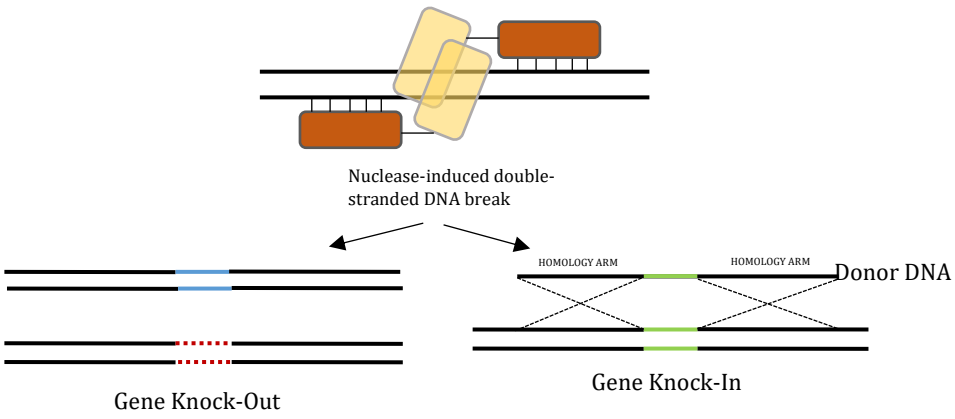

One of the first reports to demonstrate the potential of ZFNs to induce specific homology-repair mediated gene targeting in human induced pluripotent stem cells (hiPSCs) and human embryonic stem cells (hESCs) was by Zou and group (*32*) where they corrected a mutant GFP reporter gene at an efficiency of 0.14-0.24 %. Specific targeting of the *OCT4* (pluripotency-associated) gene in hESCs using zinc finger nucleases with an efficiency of 39-100 % was demonstrated (*70*). This study also reported ZFN-mediated targeting of the ubiquitously-expressed *PPP1R12C* gene and the gene encoding PITX3 transcription factor with efficiency ranges of 33-56% and ~11% in hESCs and hiPSCs, respectively.

1.5 CF Gene Therapy

Soon after the *CFTR* gene was cloned in 1989 (*59, 60, 61*), extensive research commenced to cure CF using gene therapy techniques and several studies have reported viral and non-viral techniques to facilitate CF gene therapy. Two groups (*62, 63*) demonstrated restoration of chloride ion defect using CFTR-expressing viral vectors and were among the first studies to show proof-of concept for CF gene therapy. More recently, CF gene therapy studies using adeno-associated viral vectors and lentiviral vectors (*64, 65, 66, 67*) have focused more on solving viral tropism issues and reduce host immune response, apart from trying to enhance CFTR expression levels.

In addition to delivering wild-type *CFTR*-expressing vectors, sequence-specific gene correction has also been performed. Lee *et al* (*68*) used ZFN expression plasmids and a donor plasmid containing 4.3 kb of WT CFTR sequence to repair the ΔF508 mutation and obtained an overall efficiency of < 1%. They reasoned that the low repair level was a consequence of the distance (203 bp) of the deletion mutation (CTT) from the ZFN

target site. Induced pluripotent stem cells (iPSCs) derived from CF patient fibroblasts were corrected for the ΔF508 mutation using ZFNs and a selectable plasmid donor; *in vitro* differentiation of the iPSCs towards lung lineages showed presence of fully-glycosylated CFTR protein and correction of the chloride ion defect (Crane *et al*) (*69*).

1.5.1 What Efficiency of CFTR Gene Editing is Required to Restore Therapeutically Relevant Levels of CFTR Channel Function?

It is important to note that since CF is a recessive disease, if correction is achieved in only one *CFTR* allele per cell that essentially recreates the carrier state.

Studies by Trapnell *et al.* (*52*) showed that very low levels of CFTR at 1-2 copies per cell are expressed in the human nasal, tracheal and bronchus epithelium because of the endogenous *CFTR* promoter being weak. This observation, in addition to the fact that phenotypically normal *CFTR* heterozygotes express 50% abnormal CFTR mRNA transcripts, leads to the prediction that low CFTR expression may be sufficient for restoring CF lung epithelial functions to wild-type. Johnson *et al.* (*56*) reported that as few as 6-10% corrected cells was sufficient to restore CF chloride ion transport levels to normal. A study using the *in vivo* xenograft technique showed that 5% of pseudostratified epithelial cells expressing *CFTR* corrected the CF chloride transport defect (*58*). These two studies used highly-efficient viral vector promoters to express CFTR and therefore it cannot be assured that comparable results would be obtained in differentiated human airway epithelia where *CFTR* is under the control of its endogenous promoter. To address this issue, in a set of cell mixing experiments where freshly-isolated wild-type and CF (carrying homozygous ΔF508 mutation) airway epithelial cells were mixed in varying proportions and *in vitro* differentiated using air

liquid interface method; Farmen *et al.* (*57*) demonstrated that 20% wild-type cells generated 70% trans-epithelial chloride current relative to airway epithelia containing 100% wild-type cells. This indicates that in order to correct chloride transport defect in CF cells, a small fraction of CFTR-expressing cells is sufficient (*57*). However, the clinical implications of these results are not yet known.

1.6. Objectives and Hypothesis

We hypothesize that ΔF508 gene correction in CF airway basal cells can restore normal proximal airway epithelial cell function. To test this, we aimed to accomplish the following aims:

1.6.1 Specific Aim I: Site-specific zinc finger nucleases-mediated gene correction of ΔF508 mutation in CF airway basal cells carrying ΔF508/ΔF508 mutation:

ΔF508 mutation-specific ZFNs were delivered in the form of messenger RNA (mRNA) via electroporation along with single-stranded DNA oligo (ssODN) carrying the correcting sequence to facilitate gene correction of CF airway basal cells. In order to assess the % genome modification, including % NHEJ and % gene correction, PCR followed by TIDER (Tracking of Insertions Deletions and Recombination Events) analysis and Next Generation Sequencing analysis were performed.

1.6.2 Specific Aim II: Demonstration of CFTR functional restoration in gene corrected-basal cells at the protein and ion channel function levels:

Gene corrected-airway basal cells were *in vitro* differentiated into airway pseudostratified epithelium using air liquid interface system. In order to

demonstrate restoration of CFTR ion channel function in these cells, electrophysiology analysis was performed using the Ussing chamber system. Western blot analysis was used to show presence of fully-glycosylated CFTR protein in the corrected cells.

The approach described in this study to site-specifically correct *CFTR* ΔF508 could be utilized for the following potential therapeutic approaches:

a) Edit the ΔF508 mutation in patient-derived airway basal cells *ex vivo* with an eventual aim to transplant the treated cells (as a bulk mixture of edited and non-edited cells or as expanded homogenous single-cell derived clone) back into the patient; since this is an autologous method of therapy, there is minimal risk of systemic immunological reactions in the host, (or)

b) Accomplish *in vivo* correction of ΔF508 mutation in airway basal cells.

It is important to note that since CF is a recessive disease, if correction is achieved in only one *CFTR* allele the patient would now be a CF carrier, i. e., they would be relieved from the CF symptoms.

CHAPTER 2: MATERIALS AND METHODS

2.1 Airway Basal Cells: Origin & Culturing

CF ΔF508/ΔF508 and non-CF airway basal cells were provided to us by Dr. Scott Randell (University of North Carolina, NC, USA). Basal cells were cultured on plates pre-coated with '804G-conditioned medium' and incubated at 37 ºC in humidified air with 5% CO_2. To prepare the 804G-conditioned medium, the 804G cell line (a rat bladder epithelial cell line) kindly given to us by Dr. Hongmei Mou (Massachusetts General Hospital, Boston, MA, USA) was cultured in RPMI-1640 (Sigma Aldrich) supplemented with 10 % Fetal Bovine Serum (FBS) (HyClone) and 1% Penicillin-Streptomycin (pen-strep) (Gibco) on 100 mm TC-treated culture dish (Corning®) until they were confluent. Cells were then passaged and cultured on 225cm^2 culture flask (Falcon®) at an initial seeding of 4 million cells per flask containing 50 ml medium. They were cultured at 37 ºC in humidified air with 5% CO_2. After the cells were confluent, medium was replaced with 100 ml fresh medium, and every alternate day the medium was collected and replaced with fresh medium, for up to 3 collections. Medium obtained was filter-sterilized and stored at 4 ºC.

Basal cells were cultured in either the 'dual SMAD inhibition medium (*1*) or Pneumacult™-Ex Plus medium (STEMCELL Technologies), both containing 1% pen-strep. Dual SMAD inhibition medium consisted of SAGM™ medium (Lonza) supplemented with 10 µM RhoA kinase (ROCK) inhibitor Y27362 (Reagents Direct), 1 µM A-8301 (R&D Systems), 1 µM DMH-1 (R&D Systems) and 1 µM CHIR99021 (R&D Systems); all four supplements were re-suspended in DMSO and stored at -20 ºC. Medium was replaced on a daily basis. The cells cultured in Pneumacult™-Ex Plus medium were fed fresh medium every alternate day until they reached ~50% confluence

after which they were fed daily. To passage the basal cells, they were split in the ratio 1:10 after dissociation with 0.25% trypsin (Lonza) for 5-8 minutes followed by the neutralization of trypsin by RPMI-1640 + 10% FBS.

To freeze the cells (basal or 804G), they were re-suspended in CryoStor® cryo-preservative medium (STEMCELL Technologies) and kept frozen in liquid N_2.

2.2 Characterization of Airway Basal Cells

Airway basal cells were characterized for basal cell-specific surface markers CD49f and NGFR using fluorescence analysis. 200,000 cells were incubated on ice (protected from light) for 30 minutes with αCF49f-PE (Biolegend) and/or αCD271-APC (Biolegend) (TABLE 2.1) in 100 µl of FACS buffer (phosphate buffered saline with 1% FBS). Non-immune IgG2a-PE and IgG1, κ-APC were used as isotype controls. Antibody-stained cells were washed with FACS buffer and pelleted by a 5-minute centrifugation at 200g and then re-suspended with FACS containing 0.075 µg/ml 4',6-diamidino-2-phenylindole (DAPI) (Life Technologies) for live cell separation. Two different lasers were used to excite the phycoerythrin (PE) (568 nm) and allophycocyanin (APC) (633 nm) fluors. Stained cells were analyzed on a FACS LSRII (BD Biosciences) using FACS DiVA software (BD Biosciences).

2.3 ZFN mRNA Production *In Vitro*

Exon 11 set 1 and set 2 ZFN plasmids were designed and provided by Sangamo Therapeutics and ZFN messenger RNAs (mRNAs) were synthesized by *in vitro* transcription using mMESSAGE mMACHINE™ T7 Ultra Transcription kit (Invitrogen). Briefly, template DNA was prepared by PCR amplification of 100 ng ZFN plasmid using the primers N80pt and R560 (TABLE 2.2) and enzyme AccuPrime™ *Pfx* DNA

Polymerase (Invitrogen). PCR conditions were as follows: an initial denaturation at 95 ºC for 3 minutes; 30 cycles of 95 ºC for 30 seconds denaturation, 63.6 ºC for 30 seconds annealing; 68 ºC for 2 min extension; a final extension at 68 ºC for 3 min. The PCR product was purified by Agencourt AMPure XP (Beckman Coulter) following the manufacturer's instructions. The purified PCR product was used to generate mRNA with mMESSAGE mMACHINE™ T7 Ultra Transcription kit (Invitrogen), followed by RNA purification by MEGAclear™ Transcription Clean-Up kit as per the manufacturer's instructions. The quantity and quality of the RNA was assessed by Qubit™ RNA HS Assay kit and Agilent Bioanalyzer, respectively.

TABLE 2.1 List of antibodies used for basal cell characterization

Antibody	***Company***	***Host Species***	***Catalog No.***	***Dilution***
PE antihuman/mouse CD49f Clone: GoH3	Biolegend	rat	313612	1:1000
PE isotype mouse IgG2a	Invitrogen	mouse	MG2A04	1:1000
APC anti human CD271 (NGFR) clone ME20.4	Biolegend	mouse	345108	1:1000
APC mouse IgG1,κ isotype Ctr MOPC-21	Biolegend	mouse	400121	1:1000

TABLE 2.2 List of primers used in this study

Primer Name	***Purpose***	***Primer Sequence (5' to 3')***
N80pt	ZFN mRNA production	GCAGAGCTCTCTGGCTAACTAGAG
R560	ZFN mRNA production	TTTTTTTTTTTTTTTTTTTTTTTTTTTTTTTTTTTTTTTTTTTTTTTTTTTTTTTTTTCTGGCAACTAGAAGGCACAG
#49	exon 11-Cel 1 Assay	GTAGTGTGAAGGGTTCATATGC
#50	exon 11-Cel 1 Assay	GGAGGCAAGTGAATCCTGAG
#85	PCR for Sanger Sequencing	CTATCTGAATCATGTGCCC
#88	PCR for Sanger Sequencing	TTCTCTGCTGGCAGATCAATGCTCA
CFi10a Fw	PCR for Sanger Sequencing	AGTCTATATTTGTTTTCCAGTGGC
CFi11a Rv	PCR for Sanger Sequencing	TACGAGTGGAAAAGTTGCGGA
CF5	Primer for TIDER Analysis	TGGGTAAGCTACTGTGAATG
Miseq-Fw	Primer for Next Generation Sequencing	GGGAGAACTGGAGCCTTCAG

Miseq-Rv	Primer for Next Generation Sequencing	GCATATGAACCCTTCACACTAC
CF17Fw	RT-PCR	AGGGATTTGGGGAATTATTTG
CFex1314Rv	RT-PCR	GCTGTGTCTGTAAACTGATGGCT
52-GAPDH-Fw	RT-PCR	TCTTTTGCGTCGCCAGCCGA
53-GAPDH-Rv	RT-PCR	CCTGCAAATGAGCCCCAGCC
CF1B	Allele-Specific PCR	CCTTCTCTGTGAACCTCTATCA
CF7C	Allele-Specific PCR	AGTAGAAACCACAAAGGATA
CF8C	Allele-Specific PCR	TATAGTAACCACAAAGGATA

Addition of the WPRE sequence to the ZFN plasmid was done by Dr. Ana Maria Crane, a senior research scientist in our lab. Briefly, WPRE sequence was PCR-amplified and cloned into the ZFN plasmid at XhoI and XbaI restriction enzymes site.

2.4 Transfection of Gene Editing Reagents

100 and 200-mer single-stranded oligo DNA was synthesized by Integrated DNA Technologies.

Sequence of the 100-mer ssODN (5' – 3'):

TGTTCTCAGTTTTCCTGGATTATGCCTGGCACCATTAAAGAAAATATCATCTTTGGTGTTTC CTATGATGAATATAGATACAGAAGCGTCATCAAAGCATGCC.

Sequence of the 200-mer ssODN (5' – 3'):

TCAGAGGGTAAAATTAAGCACAGTGGAAGAATTTCATTCTGTTCTCAGTTTTCCTGGATTAT GCCTGGCACCATTAAAGAAAATATCATCTTTGGTGTTTCCTATGATGAATATAGATACAGAA GCGTCATCAAAGCATGCCAACTAGAAGAGGTAAGAAACTATGTGAAAACTTTTTGATTATGC ATATGAACCCTTCA.

All the gene editing reagents (ZFN mRNAs and ssODN), and when applicable, TriLink CleanCap® EGFP (Enhanced Green Fluorescent Protein) mRNA, were transfected in to basal cells via electroporation using the BTX™ ECM 830 electroporation generator (Harvard Apparatus). The cells were harvested for electroporation using 0.25% trypsin (Lonza) (5-8 minutes), followed by the neutralization of trypsin with 10% FBS (HyClone) and then cells were washed once with phosphate buffered saline (PBS). Cells were pelleted by a 5-minute centrifugation at 200g and then re-suspended in BTXpress™ solution (Harvard Apparatus) to a final concentration of 0.5 X 10^6 cells per 100 µl of solution. Appropriate volumes of the gene targeting reagents or EGFP mRNA were added to this cell suspension and electroporation was

done in BTX™ electroporation cuvettes (2mm gap, Harvard Apparatus) at Low Voltage (LV) conditions of 250 V for 5 ms, 1 pulse. Immediately after electroporation, the cells recovered by adding 550 µl of medium (dual SMAD inhibition or Pneumacult™-Ex Plus) to the cuvette were equally distributed between 2 wells of a 6-well clear flat-bottomed plate (Falcon®) pre-coated with 804G-conditioned medium. Three days post electroporation, cells were harvested for DNA isolation, and/or expansion for further studies.

2.5 Assessment of % Genome Modification

For the Cel 1 assay (FIGURE 2.1), 100 ng genomic DNA (gDNA) isolated from transfected cells using GeneJET Genomic DNA Purification kit (Thermo Scientific) was PCR-amplified using primers #49 and #50 and the enzyme Phusion High-Fidelity DNA Polymerase (Thermo Scientific). PCR conditions were as follows: an initial denaturation at 98 ºC for 30 seconds; 35 cycles 98 ºC for 10 seconds denaturation, 68 ºC for 20 seconds annealing, 72 ºC for 15 seconds extension; a final extension at 72 ºC for 10 minutes. The PCR product was purified by Agencourt AMPure XP (Beckman Coulter). Denaturation of the amplicon at 98 ºC for 10 min was followed by re-annealing (95 ºC to 85 ºC at the rate 2 ºC per second, 85 ºC to 25 ºC at the rate 0.1 ºC per second) and subsequent incubation with surveyor nuclease enzyme (IDT) at 42 ºC for 20 min. ZFNs cause double-stranded DNA breaks (DSB) that are sealed by the cell's inherent error-prone repair mechanism termed non-homologous end joining (NHEJ) which cause nucleotide insertions and deletions (INDEL). The surveyor enzyme detects and cleaves nucleotide mismatches that results from ΔF508-INDEL or INDEl1-INDEL2 hetero-duplex formation after the denaturation-renaturation step. The cleaved DNA products were

resolved on a 10 % TBE gel (Invitrogen).

TIDER is a bioinformatics tool (https://tider.deskgen.com/) which we had used extensively in this study for the purpose of assessing % NHEJ and % gene correction. TIDER uses as its input Sanger sequence data constituting a mixture of sequences and decomposes into individual sequences with calculated frequencies (*89*). DNA from transfected and non-transfected control cells were PCR-amplified using primers CFi10aFw & CFi11aRv and after purification of PCR products (Macherey-Nagel NucleoSpin Gel and PCR Clean-Up kit), Sanger sequencing was done by Lone Star Labs (Houston, TX, USA) using the primer CF5. PCR conditions were as follows: an initial denaturation at 95 ºC for 2 minutes; 35 cycles 94 ºC for 30 seconds denaturation, 57 ºC for 30 seconds annealing, 72 ºC for 1 minute extension; a final extension at 72 ºC for 5 minutes. The 'guide sequence' for the TIDER analysis was 5'-AATATCATTGGTGTTTCCTA; control and reference chromatogram for the analyses were sequences from *CFTR* ΔF508/ΔF508 and non-CF DNA, respectively. DNA from *CFTR* ΔF508/ΔF508 and non-CF cells were PCR-amplified and sequenced together with samples in the same reaction.

Next Generation Sequencing (NGS) was done by our collaborator, Sangamo, where they used primers Miseq-Fw and Miseq-Rv for the sequencing purpose.

2.6 Isolation and Genotyping of Single-Cell Derived Clones

Flat-bottomed-96-well plate (Falcon) was first pre-coated with 1% collagen (PureCol ® from Advanced BioMatrix), after which 30,000 ATCC-irradiated NIH3T3 fibroblasts per well per 30 µl of complete DMEM medium was added. Complete DMEM medium included DMEM (Gibco), 10% FBS (HyClone), 1 % pen-strep and 1 %

GlutaMAX (Gibco). The next day, to each well containing mouse fibroblast feeder layer, airway basal cells were added at the cell density of 1 cell per well or 5 cells per well and cultured thereafter in the conditionally-reprogrammed cell (CRC) medium at 37 ºC in humidified air with 5% CO_2. CRC medium was composed of complete DMEM medium, F-12 Nutrient Mix (Gibco), hydrocortisone (Sigma) (25 ng/ml), EGF (Invitrogen) (0.125 µg/ml), insulin (Sigma) (5 µg/ml), fungizone/amphotericin B (Fisher) (250 ng/ml), Gentamicin (Gibco) (10 µg/ml), cholera toxin (Sigma) (0.1 µM) and ROCK inhibitor Y-27362 (Reagents Direct) (10 µM). The cells were monitored daily to confirm that a basal cell colony emerged from single cell and the wells that contained multiple colonies were omitted from further studies. After 5-8 days of initial seeding, when single-cell clones were greater than 50 % confluent, they were harvested using the method of differential trypsinization, which involved initial trypsinization using 0.05 % trypsin (Gibco) for 15-30 seconds to detach and remove the fibroblasts, followed by detachment of basal cell clones using 0.25% trypsin (Gibco) for 5-8 minutes. Each clone was then seeded on to one well of an 804G-coated 48-well plate (Falcon) and cultured in the dual SMAD inh medium. After they were ~70% confluent, each clone was replicated into one well of a 48-well plate (Falcon) (1:4) and one well of a 12-well plate (Falcon) (3:4). The cells from the 48-well plate were harvested for DNA isolation and subsequent allele-specific PCR (AS-PCR) and Sanger sequencing analyses

For AS-PCR, 100 ng DNA (isolated using Macherey-Nagel NucleoSpin Tissue XS kit) from each clone was PCR-amplified using the primer pairs CF1B/CF7C (wild-type-specific) and CF1B/CF8C (ΔF508 mutant-specific) and MyTaq™ polymerase enzyme mix (Bioline). The PCR conditions were as follows: initial denaturation at 95 ºC for 2

FIGURE 2.1 Schematic of Cel 1 Assay: *Three days post-transfection with ZFN, DNA PCR amplification followed by denaturation and subsequent renaturation results in DNA mismatches (as a result of ΔF508-INDEL or INDEL1-INDEL2 hetero-duplex formation) that are detected and cleaved by surveyor nuclease enzyme. Shown in red and blue are insertions and deletions (INDELs) resulting from the DSB induced by ZFNs followed by the error-prone NHEJ DNA repair mechanism in cells.*

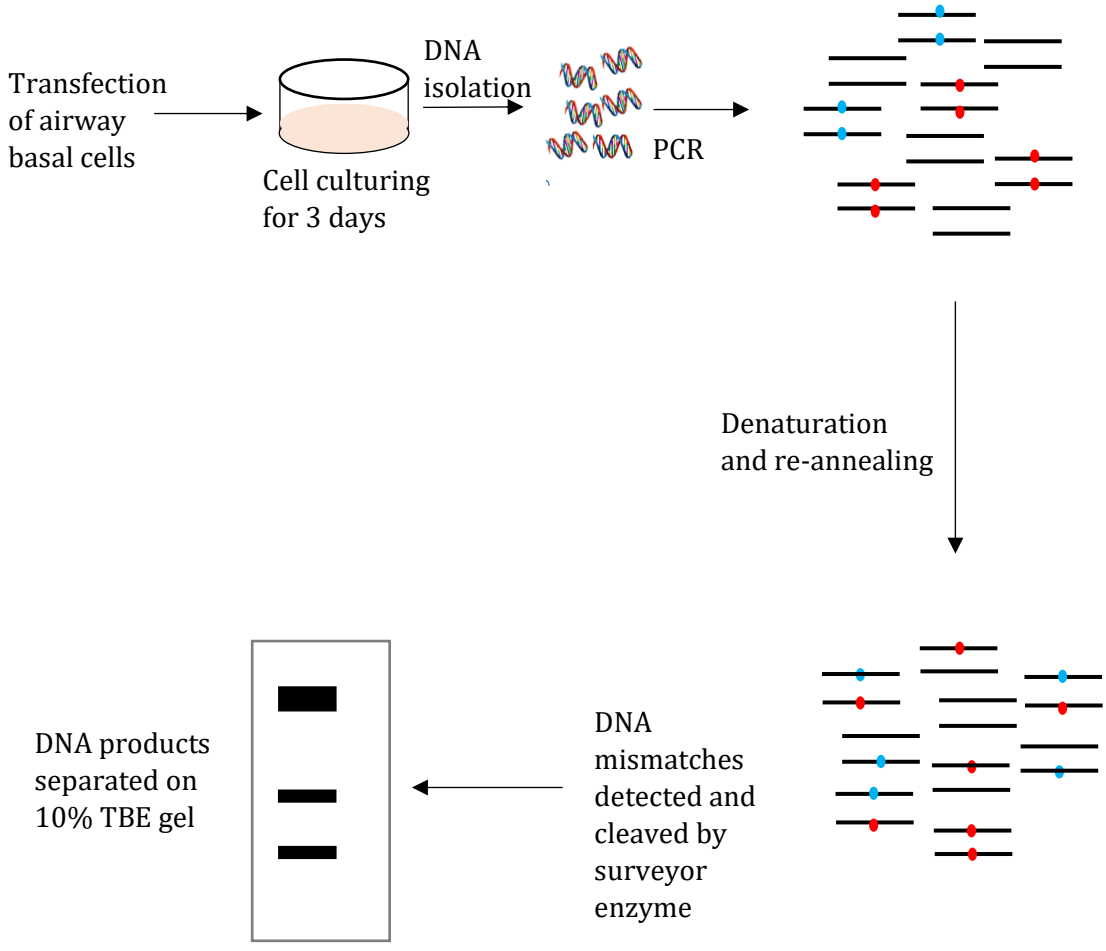

minutes; 35 cycles of 95 ºC for 30 seconds denaturation, 60 ºC for 30 seconds annealing, 72 ºC for 1 minute extension; a final extension at 72 ºC for 5 minutes. The PCR amplicon products were separated on a 1.4% agarose gel

For the purpose of Sanger sequencing, 100 ng DNA from each clone was PCR-amplified using the primers #85 and #88 and GoTaq™ Hot Start polymerase enzyme mix (Promega). The PCR conditions were as follows: initial denaturation at 95 ºC for 2 minutes; 35 cycles of 94 ºC for 30 seconds denaturation, 57 ºC for 30 seconds annealing, 72 ºC for 1 minute extension; a final extension at 72 ºC for 5 minutes. The amplicon products were purified using Nucleospin® Gel and PCR clean-up kit (Macherey-Nagel) and Sanger sequencing was done by Lone Star Labs (Houston) using primer #88.

2.7 *In vitro* Differentiation of Basal Cells by Air Liquid Interface (ALI) System

Airway basal cells were seeded on to the top chamber of a 6.5 mm Transwell® with 0.4 µm pore polyester membrane inserts (Corning) which were pre-coated with 804G-conditioned medium. 200,000 cells was initially seeded and were cultured in dual SMAD inhibition or Pneumacult™-Ex Plus medium, added to the top and bottom chambers until the cells were 100% confluent after which, medium was replaced by Pneumacult-ALI medium (Stemcell Technologies) containing 1% pen-strep (Gibco). The next day, medium from the top chamber was removed to establish air-liquid interface and the cells were cultured this way for 4 weeks with daily feeding.

2.8 CFTR RT-PCR

Total RNA was isolated from ALI-cultured cells using NucleoSpin RNA Plus kit (Macherey-Nagel) and cDNA synthesis was done using ImProm-II reverse transcriptase

(ImProm-II Reverse Transcription System, Promega) after combining RNA with Oligo$(dT)_{15}$ primer. CFTR RT-PCR was performed with primers CF17Fw and CFex1314Rv and AccuPrime™ *Pfx* DNA Polymerase enzyme. RT-PCR of GAPDH with primers 52-GAPDH-Fw and 53-GAPDH-Rv was done as a control. PCR conditions were as follows: an initial denaturation at 94 ºC for 2 minutes; 35 cycles 94 ºC for 15 seconds denaturation, 55 ºC for 15 seconds annealing, 68 ºC for 45 seconds extension; a final extension at 68 ºC for 2 minutes.

2.9 Histology and Immunofluorescence Studies

Hematoxylin & eosin (H&E) staining was done by Dr. Zhengmei Mao (Microscopy Core Facility, UTHealth).

Immunofluorescence study was performed on cryo-section of cells cultured in air-liquid interface membrane inserts. Briefly, the samples were fixed with 4 % paraformaldehyde (PFA) (Electron Microscopy Sciences) in PBS at 4 ºC overnight after thorough washing with PBS. The cells were then washed thrice with ice-cold PBS, 5 min each. After cryopreservation using sequential sucrose treatment (first 15%, then 30 % sucrose in PBS, for 60 min each), the insert, after removal from the transwell using a clean surgical blade, was incubated in OCT embedding medium (Fisher) for 5 min and then transferred into a cryomold (Andwin Scientific) and flash frozen in OCT with dry ice. Sectioning was performed (5-8 µm) using Leica® CM1850 Cryostat and the cryo-section was dried overnight. For immunostaining, the sectioned samples were first hydrated with PBS (5 min), permeabilized with 0.25 % Triton X-100 (Sigma) in PBS for 15-30 min and blocked with 2 % bovine serum albumin (BSA) for 1 hour. Samples were then incubated with primary antibodies in 2 % BSA (TABLE 2.3) overnight at 4 ºC,

followed by three washes with PBS, 5 min each. They were then incubated with the respective secondary antibodies in 2 % BSA (TABLE 2.4) at room temperature for two hours. Followed by three 5 minute-washes in PBS, Prolong™ Gold Antifade Mountant with DAPI (Invitrogen) was added to counter-stain and mount the samples and the samples were cured for 24 hours. For H&E and immuno-staining, images were acquired using Leica DMi8 microscope (Leica Microsystems) and Leica Application Suite Software (Leica Microsystems).

For the purpose of relative quantification of the epithelial cell type, for each antibody staining, images were captured from three random fields. In each of the field, the number of each cell type (indicated by their respective immunostaining) was counted relative to the total number of cells (indicated by nuclei staining by DAPI).

2.10 CFTR Western Blot Analysis

ALI-cultured cells were lysed using RIPA Lysis and Extraction Buffer (Pierce) after washing the inserts thoroughly with PBS. To obtain protein extracts, the cells were flash frozen and thawed twice, and centrifuged at 3000 g for 10 min (4 ºC) to collect the supernatant containing protein. The protein concentration was determined using the colorimetric BCA assay (Pierce). The protein samples were then prepared for separation by gel electrophoresis in the following way: Sample Reducing Agent (NuPAGE) and Sample Buffer (NuPAGE) was added to 60 µg of the protein supernatant, and the total volume was made up to 50 µl with RIPA buffer (Pierce). NuPAGE 7 % Tris-Acetate Protein Gels were used to resolve the proteins, 5 µl of protein ladder (Precision Plus Protein™ Dual Color Standards, Biorad) was loaded in to the gel. SDS Running Buffer (NuPAGE) was added to the outer chamber and running

FIGURE 2.2 Schematic of air-liquid interface differentiation

(a) *Basal cells were seeded on to membrane inserts with 0.4 µm pores and cultured in dual SMAD inhibition or Pneumacult-Ex plus medium (orange) on the top and bottom chambers until they were 100% confluent, after which* ***(b)*** *medium was replaced by Pneumacult-ALI medium (yellow).* ***(c)*** *The next day, medium from the top chamber was removed to establish air-liquid interface and the cells were cultured this way for 4 weeks.*

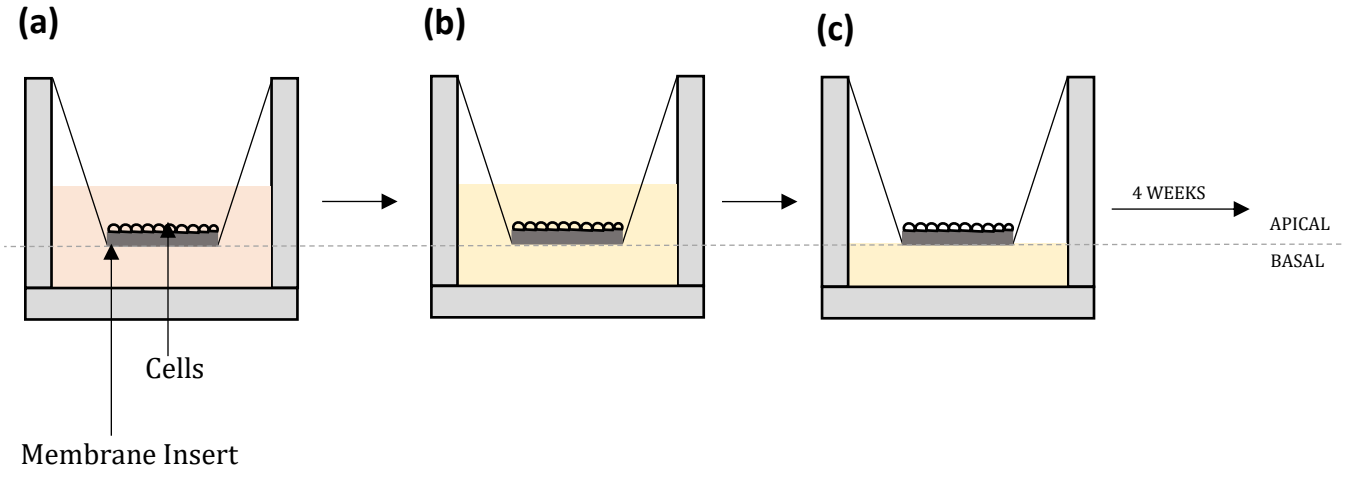

TABLE 2.3 List of primary antibodies used in immunofluorescence or Western blot analysis of ALI-cultured cells

Antibody	***Company***	***Host Species***	***Clone***	***Dilution***
FOXJ1	Invitrogen	Mouse	2A5	1:200
FOXI1	Sigma	Rabbit	polyclonal	1:200
ACT	Sigma	Mouse	6-11B-1	1:1000
p63	Biocare	Mouse	4A4	1:100
CK5	CST	Rabbit	D4U8Q	1:200
MUC5AC	Thermo Scientific	Mouse	45M1	1:200
CFTR 596	Cystic Fibrosis Foundation	Mouse	A4	1:1000
Calnexin	Abcam	Rabbit	polyclonal	1:2000

TABLE 2.4 List of secondary antibodies used in immunofluorescence or Western blot analysis of ALI-cultured cells

Antibody	*Host Species*	*Company*	*Dilution*	*Fluorophore*
goat anti-mouse	goat	Invitrogen	1:500	Alexa555
goat anti-mouse	goat	Invitrogen	1:500	Alexa488
goat anti-rabbit	goat	Invitrogen	1:500	Alexa555
goat anti-rabbit	goat	Invitrogen	1:500	Alexa488
donkey anti-mouse	donkey	Invitrogen	1:500	Alexa555

buffer + antioxidant (NuPAGE) was added to the inner chamber of the electrophoresis apparatus. The gel was run for 60 min at 60 V, and then at 100 V for 3 hours. Resolved proteins on the gel was transferred onto Hybond-C nitrocellulose transfer membrane (Amersham Bioscience) and blocked with 5% non-fat dry milk (in PBS) (blocking buffer) at room temperature for 30 minutes. The membrane was then incubated with CFTR primary antibody mIgG2b 596 (1:1000; Cystic Fibrosis Foundation Therapeutics) in blocking buffer overnight at 4 ºC. After that, the membrane was washed 4 times with TBS + 0.1 % Tween 20 + blocking buffer (5 min per wash). This was followed by incubation in secondary antibody HRP-linked anti-mouse (1 : 5000, Cell Signaling Technologies) in blocking buffer overnight at at 4 ºC, subsequent washing 4 times with TBS + 0.1 % Tween 20 + blocking buffer (5 min per wash) and detection by chemiluminescense using Amersham ECL Prime.

2.11 Ussing Chamber Analysis

Ussing chamber electrophysiology analyses was done by Dr. Andras Rab (Dr. Eric Sorscher lab, Emory University), our collaborator. In brief, membrane inserts were mounted in Ussing chambers and chloride ion gradient was established by providing low chloride Ringer solution on the apical side, regular Ringer solution on the basolateral side. Compounds were added in the following order: 1) amiloride for 10 minutes (100 µM), apical and basolateral side, 2) forskolin for 5 minutes (10 µM), apical and basolateral side, 3) CFTR inhibitor-172 (10 µM), apical side, and 4) UTP (100 µM), apical side. The resulting changes in short-circuit current was calculated as ΔI_{sc}.

2.12 Statistical Analysis

We used Microsoft Excel (Seattle, WA, USA) for all our statistical analysis. The

Student's t test was used to determine significance between test and control groups. *P*-value < 0.05 were considered statistically significant.

CHAPTER 3: RESULTS

3.1 Airway Basal Cell Characterization

Airway basal cells express characteristic cell surface markers such as CD49f and NGFR. We confirmed the cell surface phenotype of our cultured non-CF and ΔF508/ΔF508 airway basal cells by staining with CD49f and CD271 (NGFR) antibodies and fluorescence analysis (FIGURE 3.1). The staining patterns were consistent with pure basal cell populations.

3.2 Analysis of Zinc-Finger Nuclease (ZFN) Activity in Airway Basal Cells

Two sets of zinc finger nucleases (ZFNs) (namely 'exon 11 set 1 ZFN' and 'exon 11 set 2 ZFN') specific to the *CFTR* ΔF508 sequence were designed and provided to us as plasmid DNA by Sangamo Therapeutics through a collaboration. Each ZFN monomer (eg: ZFN-L or ZFN-R) consists of a DNA-binding domain and a FokI-endonuclease domain, and following binding of ZFNs to targeted DNA sequences, dimerization results in a double-stranded DNA break (DSB). Exon 11 ZFN sets 1 and 2 include a common ZFN-left (ZFN-L) component with the DNA-binding domain specific for *CFTR* ΔF508, but not wild-type exon 11 sequence. Each of the ZFN-right (ZFN-R) components of 1 and 2 recognizes the same target sequences but differ in the amino-acid composition (FIGURE 3.2). Achieving reasonable levels of gene correction of *CFTR* ΔF508 mutation via HDR pathway of the cell requires that ZFNs efficiently induce the DSB. Therefore, we tested the efficiency of cutting by the ZFNs by assessing the % NHEJ (non-homologous end joining), also denoted as % INDEL.

The ZFNs were delivered via electroporation to the cells in the form of messenger

FIGURE 3.1 Basal cell characterization. *Basal cells cultured in 'dual SMAD inhibition' medium were characterized for basal cell-specific surface markers CD49f and NGFR using fluorescence analysis. They were found to be double positive for the two markers (Q2) consistent with being pure basal cell populations.* ***A)*** *non-CF cells at passage 5.* ***B)*** CFTR *ΔF508/ΔF508 cells at passage 6.*

A)

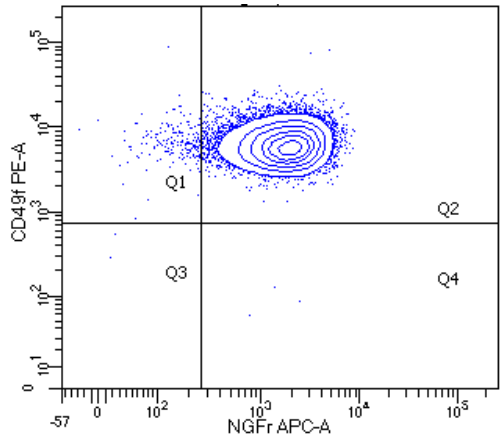

B)

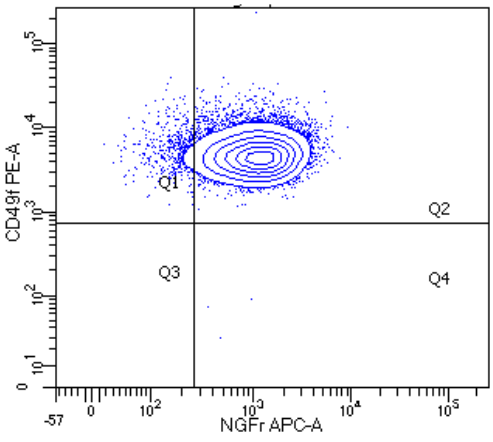

RNA (mRNA). ZFN plasmids were used as DNA templates for *in vitro* production of their respective ZFN mRNA generated by *in vitro* transcription using the T7 promoter. Sangamo Therapeutics published a report wherein they showed that inclusion of the woodchuck hepatitis virus post-transcriptional response element (WPRE) in the 3' UTR of ZFN mRNA enhanced protein expression of the nuclease and also increased cutting efficiency (*71*). The WPRE sequence increases protein expression by increasing mRNA stability and/or increased translation. We therefore assayed the efficiency of the exon 11 set 1 and 2 ZFNs with and without WPRE. After three days of culturing the cells post electroporation, the cells were harvested for genomic DNA (gDNA) isolation. The Cel 1 assay was performed as a qualitative test to check for ZFN activity. Briefly, PCR amplification of the region surrounding the cut site followed by subsequent denaturation and renaturation of the amplicon resulted in sequence mismatches (eg: INDEL-ΔF508 and/or INDEL1/INDEL2) which were detected and cleaved by surveyor nuclease enzyme. The resulting digested DNA was resolved by gel electrophoresis (FIGURE 3.3). An accurate determination of % NHEJ was obtained by high-throughput Next Generation Sequencing (NGS) analysis (by our collaborator, Sangamo Therapeutics). These data showed that indeed, addition of the WPRE sequence improved efficiency of ZFN cleavage (~ 4 – 12 fold) (FIGURE 3.3). The dose responsiveness of ZFN mRNA with WPRE sequence was assessed in two independent experiments and the data showed an increase in % cutting with increase in ZFN amount (FIGURE 3.4).

FIGURE 3.2 A) *Each ZFN monomer includes a DNA-binding domain (blue and orange) and a FokI-endonuclease domain (green). After binding of the FokI domains, dimerization results in double-stranded DNA breaks (DSB).* ***B)*** *Shown in blue and orange are the sequences to which* CFTR *exon 11 ZFN-L and ZFN-R bind, respectively. ZFN-L is specific to the* CFTR *ΔF508 mutant sequence.*

A)

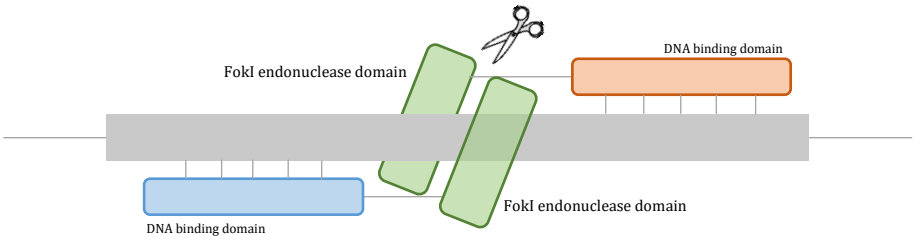

B)

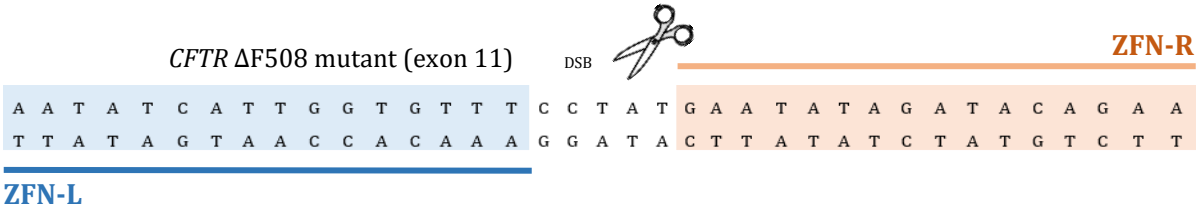

FIGURE 3.3 % NHEJ resulting from the action of ZFN mRNA +/- WPRE sequence. A) *Primers for Cel 1 assay are shown in purple (forward primer) and green (reverse primer). Approximate DNA cut site is indicated by a pair of scissors. The resulting DNA sizes upon cleavage of mismatches (eg: INDEL-ΔF508 and/or INDEL1/INDEL2) by surveyor nuclease are ~ 300 and ~100 bp. In an experiment to compare % cutting efficiency by ZFN +/- WPRE, 4 µg each ZFN mRNA was transfected in to 0.5 million basal cells.* ***B)*** *Results of Cel 1 assay. The presence of cleaved DNA indicates ZFN-induced INDELs activity.* ***C)*** *NGS analysis quantified the % NHEJ resulting from the action of ZFN +/- WPRE. DNA from non-transfected cells (no ZFN) was used as a negative control.*

A)

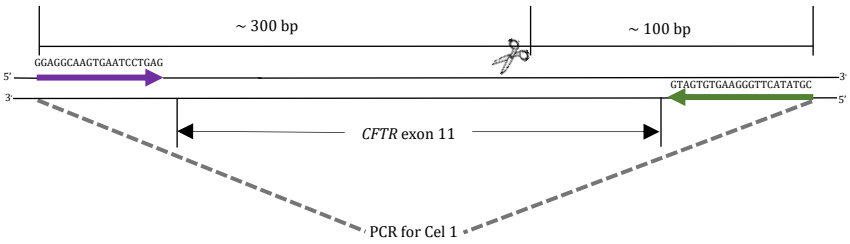
~ 300 bp
~ 100 bp
GGAGGCAAGTGAATCCTGAG
GTAGTGTGAAGGGTTCATATGC
5'
3'
3'
5'
CFTR exon 11
PCR for Cel 1

B)

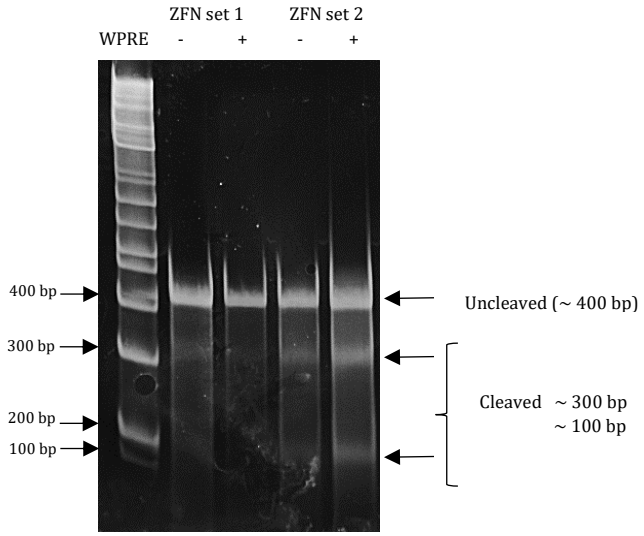
ZFN set 1
ZFN set 2
WPRE - + - +
400 bp
300 bp
200 bp
100 bp
Uncleaved (~ 400 bp)
Cleaved ~ 300 bp
~ 100 bp

C)

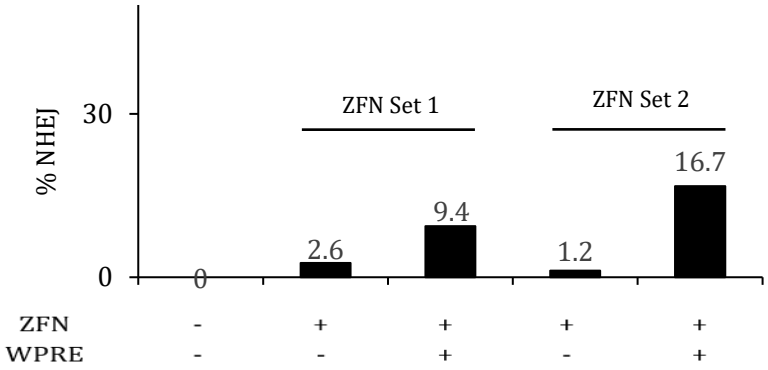
% NHEJ
30
0
ZFN Set 1
ZFN Set 2
0
2.6
9.4
1.2
16.7
ZFN - + + + +
WPRE - - + - +

FIGURE 3.4 Dose response curve of ZFN + WPRE mRNA.

Two independent experiments were conducted to assess % NHEJ resulting from the action of varying doses of ZFN + WPRE mRNA. ***A)*** *EXPT 1: Results from NGS analysis. % NHEJ was found to increase with ZFN amount for both ZFN set 1 and set 2.* ***B)*** *EXPT 2: Results from NGS analysis. Similar to that seen in experiment 1, % cutting increased with ZFN dose. DNA from non-transfected cells were used as negative controls in both experiments.*

A)

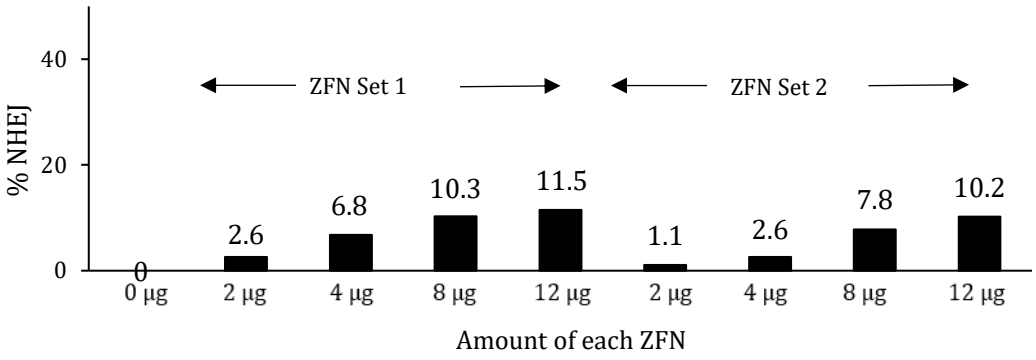

B)

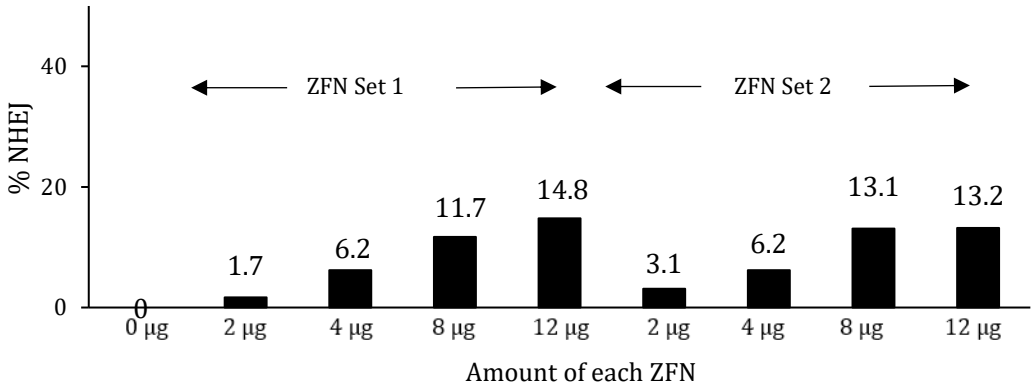

We noticed variation in % NHEJ between experiments and reasoned that it may be due to a difference in quality of the mRNA synthesized by *in vitro* transcription for each experiment. Therefore, we purchased large-scale *in vitro* transcribed ZFN mRNA from TriLink Technologies. Exon 11 ZFN set 1 +WPRE (since we did not see much difference between the efficiency of set 1 and set 2 ZFNs) was manufactured using the plasmid template that we provided to TriLink and this was used in our subsequent experiments. To test the efficiency of the commercially-synthesized ZFN, we performed a transfection experiment in which varying doses of ZFNs were tested (0.5 - 16 µg each ZFN) and % NHEJ was assessed by NGS (FIGURE 3.5).

3.3 Gene Correction of *CFTR* ΔF508/ΔF508 Airway Basal Cells

As noted earlier, gene correction is dependent upon the induction of a DSB resulting from the action of ZFNs and the introduction of template DNA carrying the correcting sequence. Gene correction of ΔF508 would be evidenced by the addition of three bases (CTT) in exon 11 of *CFTR.* We tested the individual efficiencies of a 100 and a 200-mer single-stranded oligo donor DNA (ssODN) to facilitate ZFN-mediated correction of the *CFTR* ΔF508 mutation. The 100-mer ssODN and the 200-mer ssODN had 50 base homology and 100 base homology on each side of the ZFN cut site, respectively (FIGURE 3.6a). In cells receiving 4 µg of each ZFN with either ~2 X 10^8 or ~4 X 10^8 copies of ssODN per cell, % genome modification was assessed 3 days post-transfection using NGS. With 2 X 10^8 per cell, % gene correction of 1.3 and 8.1 was obtained using the 100 and 200-mer ssODN, respectively. With 4 X 10^8 copies per cell, we obtained a % gene correction of 3.3 and 9.8 using the 100 and 200-mer ssODN, respectively (FIGURE 3.6b). This experiment indicated that the 200-mer

FIGURE 3.5 Dose response curve of commercially (Trilink)* in vitro *transcribed ZFN + WPRE mRNA. *We tested the efficiency of TriLink ZFN mRNA using different amounts. Negative controls were DNA from non-transfected cells and cells transfected with 0.5 µg GFP mRNA. We suspect that decreased % NHEJ for 12 µg was perhaps due to experimental error of some kind.*

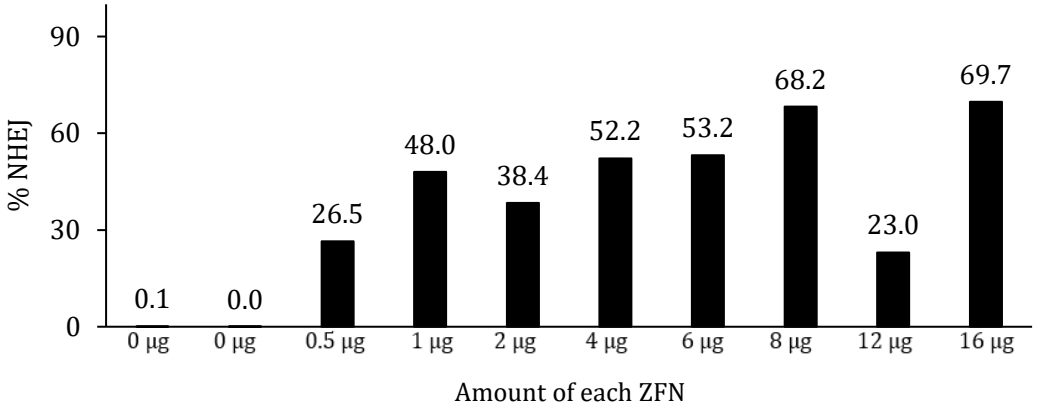

ssODN resulted in higher % gene correction. We thus proceeded with only the 200-mer ssODN.

3.4 Assessment of CFTR Functional Restoration in Gene Corrected Cells

In a subsequent experiment where ~ 4 X 10^8 copies per cell of the 200-mer ssODN (20 µg) and 4 µg of each ZFN mRNA were transfected into cells in duplicate reactions (samples denoted as 'corrected 1' (C1) and 'corrected 2' (C2)), Gene correction frequencies of 15.3% and 17.5% were measured at day 3 post electroporation (FIGURE 3.7). These cells were further expanded and assessed for CFTR functional restoration.

Basal cells do not express CFTR and therefore the corrected cells were differentiated *in vitro* using the air liquid interface (ALI) system to give rise to differentiated epithelium expressing CFTR. Briefly, basal cells were first cultured on 6.5 mm Transwell® with 0.4 µm pore polyester membrane insert (Corning) at an initial density of ~6000 cells/mm^2 in dual SMAD inh medium. After the cells were confluent, medium was replaced in the top and bottom chamber with Pneumacult™-ALI medium. The next day, medium was removed from the upper chamber and the cells were cultured this way for 28 days with daily medium replacement.

We observed a decrease in the % genome modification (including both % gene correction and % NHEJ) from cells harvested three days post-transfection ('day 3' data) (e.g.: C1: 68.2 % NHEJ, 15.3 % correction) to those harvested after further expansion ('day 7' data) (e.g.: C1: 58.6 % NHEJ, 8.8 % correction). We also noticed that the

FIGURE 3.6 Gene correction of* CFTR *ΔF508/ΔF508 basal cells. A) *The three-base deletion (CTT) (i. e. the* CFTR *ΔF508 mutation) is shown in red. We tested the individual efficiencies of 100- and 200-mer ssODNs to facilitate ZFN-mediated* CFTR *gene correction. Blue indicates corrected sequence.* ***B)*** *Results from NGS analysis to assess % NHEJ and % gene correction by the ZFN mRNA and 100 or 200-mer ssODN. The 200-mer ssODN was found to be more efficient.*

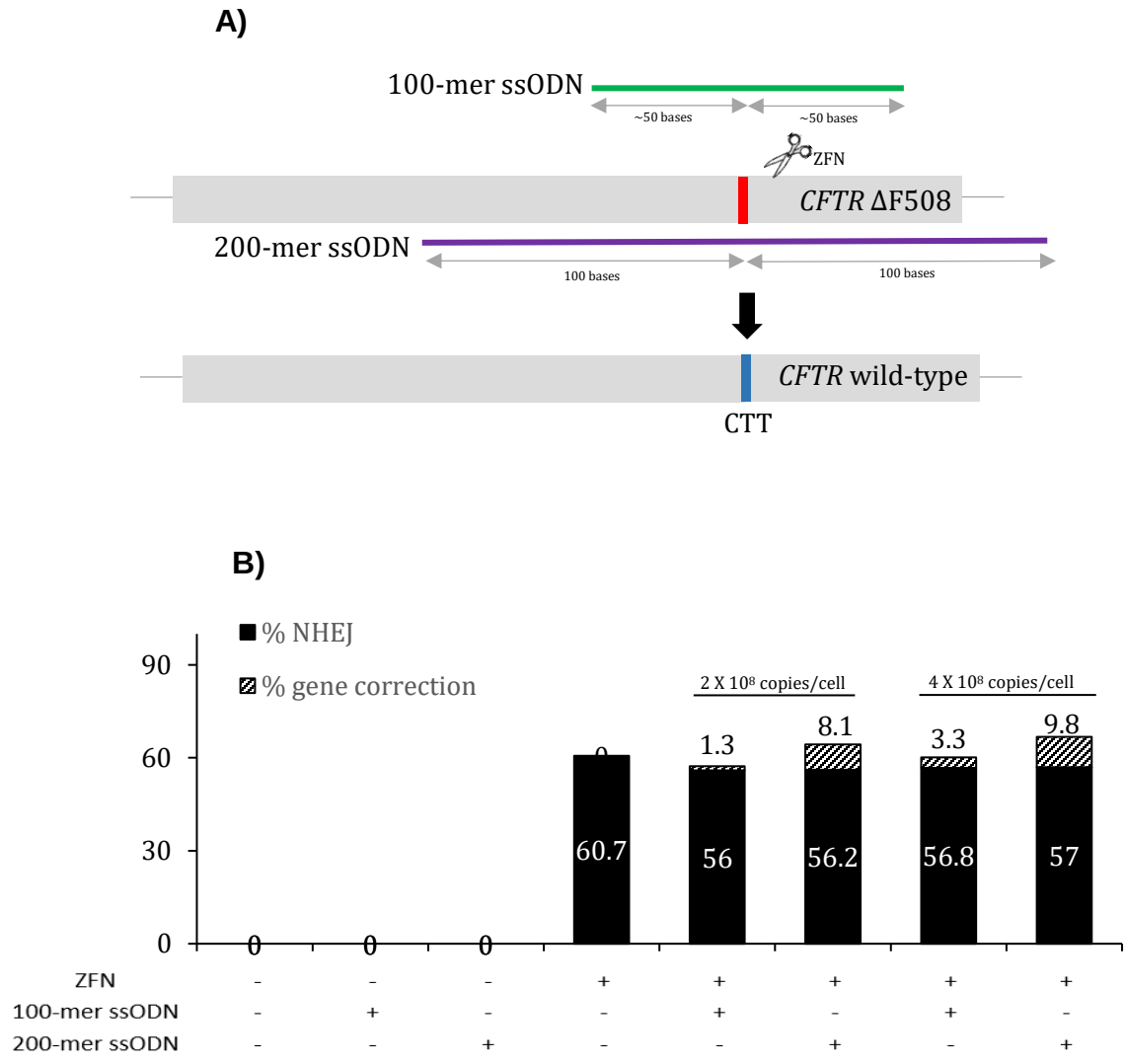

values obtained in the latter case was more similar to that obtained after 4 weeks of ALI differentiation (e.g.: C1: 58.8 % NHEJ, 10.7 % correction) (FIGURE 3.7).

RNA was isolated from the ALI-differentiated cells and subsequent complementary DNA (cDNA) synthesis followed by reverse-transcriptase PCR (RT-PCR) was performed using primers specific to the *CFTR* cDNA. In the two gene-corrected samples (C1, C2), as well as in the mutant controls (with ZFN or oligo), the *CFTR* cDNA was observed to be present. This was as expected since the ΔF508 mutants synthesize *CFTR* mRNA; it is only that protein processing (glycosylation, maturation and transport) are impaired. The gene correction frequency for C1 was quite similar for cDNA (10.5%) and gDNA (10.7%). Greater differences were observed for C2 (8.5% for cDNA and 11.1% for gDNA). We have not investigated the reason(s) for similarity versus differences between % efficiencies in cDNA versus gDNA.

Ussing chamber electrophysiology studies were performed (by our collaborators, Drs. Andras Rab and Eric J. Sorscher, Emory University) to assess CFTR functional restoration in the *in vitro*-differentiated corrected cells. In the experiment with samples C1 and C2, ΔI_{sc} upon forskolin treatment was measured as 3.2 and 4.7 μA/cm^2, respectively (and treatment with $CFTR_{inh}$-172 gave ΔI_{sc} values of -3.3 and -4.4 μA/cm^2, respectively). The forskolin-induced values were higher than in the mutant controls ($p < 0.05$) (FIGURE 3.9). In comparison, non-CF cells showed ΔI_{sc} values of 13.1 μA/cm^2 and -17.3 μA/cm^2 upon forskolin and CFTR-inhibitor treatment, respectively. Together, this data shows that even modest efficiencies of *CFTR* gene correction result in observable restoration of CFTR ion channel activity.

FIGURE 3.7 Gene correction experiment with 4 µg each ZFN and 20 µg of the 200-mer ssODN: A) *Timeline showing analyses done post transfection.* ***B)*** *0.5 million cells at passage 5 were transfected. We obtained 15.3 and 17.5 % in two treated samples (denoted as 'corrected 1' (C1) and 'corrected 2' (C2)) as assessed three days-post transfection (day 3). The total % genome modification decreased from day 3 to day 7 (i. e. to 8.8% and 11.3% respectively), but the values obtained on day 7 were maintained through ALI-differentiation (ALI diff.). Negative control included DNA from non-transfected mutant cells (no ZFN no ssODN), expanded and differentiated at the same time as the test samples.*

A)

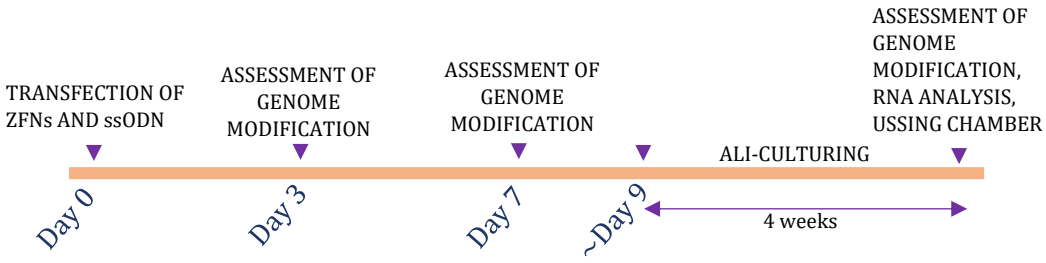
TRANSFECTION OF ZFNs AND ssODN
ASSESSMENT OF GENOME MODIFICATION
ASSESSMENT OF GENOME MODIFICATION
ASSESSMENT OF GENOME MODIFICATION, RNA ANALYSIS, USSING CHAMBER
ALI-CULTURING
Day 0
Day 3
Day 7
~Day 9
4 weeks

B)

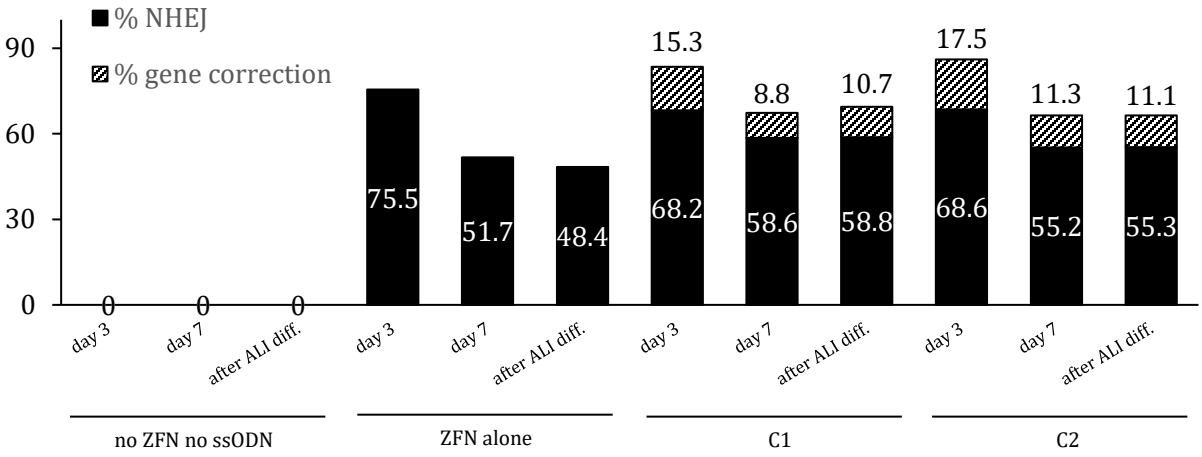
% NHEJ
% gene correction
90
60
30
0
0
0
0
75.5
51.7
48.4
15.3
68.2
8.8
58.6
10.7
58.8
17.5
68.6
11.3
55.2
11.1
55.3
day 3
day 7
after ALI diff.
day 3
day 7
after ALI diff.
day 3
day 7
after ALI diff.
day 3
day 7
after ALI diff.
no ZFN no ssODN
ZFN alone
C1
C2

FIGURE 3.8. RNA analysis of ALI-cultured cells. A) CFTR *RT-PCR: Forward and reverse primers flanked exons 10 & 11, and exons 13 & 14, respectively. Expected band size was 581 bp.* ***B)*** GAPDH *RT-PCR: Expected band size was 379 bp. 'RT-PCR controls' for both included PCR reactions without any cDNA template.* ***C)*** *Results from NGS analyses of the gDNA and cDNA 4 weeks post-ALI differentiation. gDNA from ALI-differentiated non-transfected mutant cells (no ZFN no ssODN) was used as a negative control here. We do not yet have an explanation for the differences in % NHEJ in gDNA versus cDNA for sample C1 and the differences in % gene correction in DNA versus cDNA for sample C2*

A)

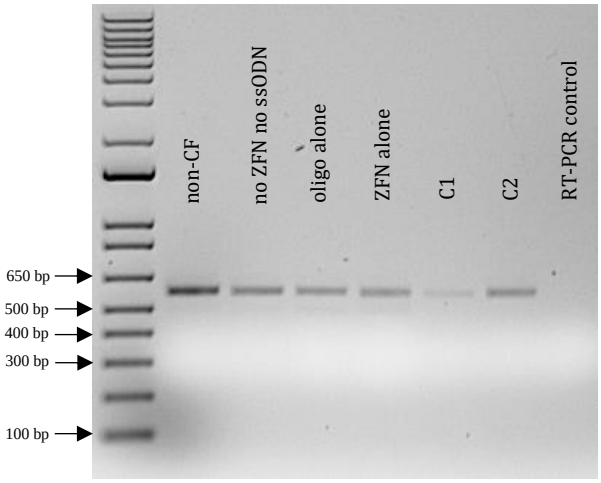
non-CF
no ZFN no ssODN
oligo alone
ZFN alone
C1
C2
RT-PCR control
650 bp
500 bp
400 bp
300 bp
100 bp

B)

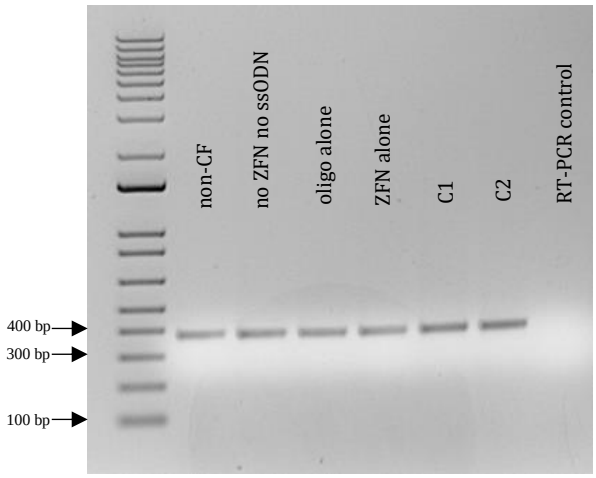
non-CF
no ZFN no ssODN
oligo alone
ZFN alone
C1
C2
RT-PCR control
400 bp
300 bp
100 bp

C)

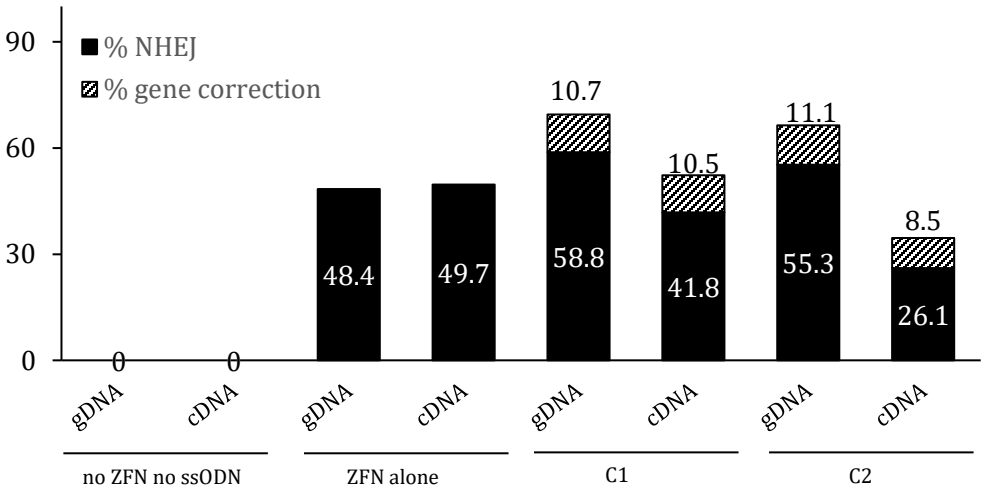
90
60
30
0
% NHEJ
% gene correction
0
0
48.4
49.7
58.8
10.7
41.8
10.5
55.3
11.1
26.1
8.5
gDNA
cDNA
gDNA
cDNA
gDNA
cDNA
gDNA
cDNA
no ZFN no ssODN
ZFN alone
C1
C2

3.5 Isolation of Single-Cell Clones from Bulk-Corrected Basal Cells

We then performed single-cell clonal isolation from the bulk population of gene-corrected basal cells using the conditionally-reprogrammed culture (CRC) methodology (*72*). Briefly, the CRC methodology involves co-culturing of airway basal cell on a feeder layer of irradiated mouse fibroblasts together with ROCK inhibitor Y-27362. The combination of the fibroblast feeder layer and ROCK inhibitor helps maintain basal cell characteristics such as self-renewal, differentiation potential and clone forming ability (*73*).

In our single-cell clonal isolation experiment, we seeded a single basal cell from the C2 corrected cell population (refer SECTION 3.4 and FIGURE 3.7) into each well of a 96-well plate containing 30,000 irradiated fibroblasts. Each well was closely monitored daily for the appearance of a single-cell derived colony (wells with more than one colony were discontinued for further studies). After single-cell derived colonies were greater than 50 % confluent, they were isolated using differential trypsinization technique to avoid contamination by the fibroblast cells. The isolated basal cells were further expanded in dual SMAD inh medium and studied. 60 single-cell clones were isolated, out of which 45 reached senescence before they could be analyzed further. The remaining 15 clones proliferated up to a time point where their DNA could be analyzed, but they also experienced eventual growth arrest by senescence. We first screened the 15 clones by allele-specific PCR (AS-PCR) using the primer pairs CF1B/CF7C (wild-type-specific) and CF1B/CF8C (ΔF508-mutant-specific) (FIGURE 3.10). This was followed by Sanger sequencing analyses (FIGURE 3.11). Out of the 15 clones that were sequenced, 1 was WT/INDEL (clone #27), 5 were INDEL/INDEL, 3 were INDEL/ΔF508,

FIGURE 3.9 Ussing chamber analysis of ALI-cultured cells. *After 4 weeks of ALI differentiation, Ussing chamber assays were performed for samples C1 and C2 together with controls. Negative controls included no ZFN no ssODN and ssODN-alone transfection controls and ZFN-alone control. Non-CF cells were used as a positive control. All controls were at the same passage and were differentiated at the same time as the test samples.* ***A)*** *Upon forskolin activation, the* ΔI_{sc} *in the treated samples C1 and C2 were calculated to be 3.2 and 4.7* $\mu A/cm^2$*, respectively. These values were significantly different (*$p < 0.05$*) when compared with the negative controls.* ***B)*** $CFTR_{inh}$*-172* ΔI_{sc} *values were determined to be -3.3 and -4.4* $\mu A/cm^2$ *for samples C1 and C2, respectively. These values were significantly different (*$p < 0.05$*) when compared with the negative controls. Data are presented as mean ± SD, 8 membrane inserts for each condition were analyzed (n=8).* * $P < 0.05$ *versus no ZFN no ssODN mutant control. NS indicates non-significant.*

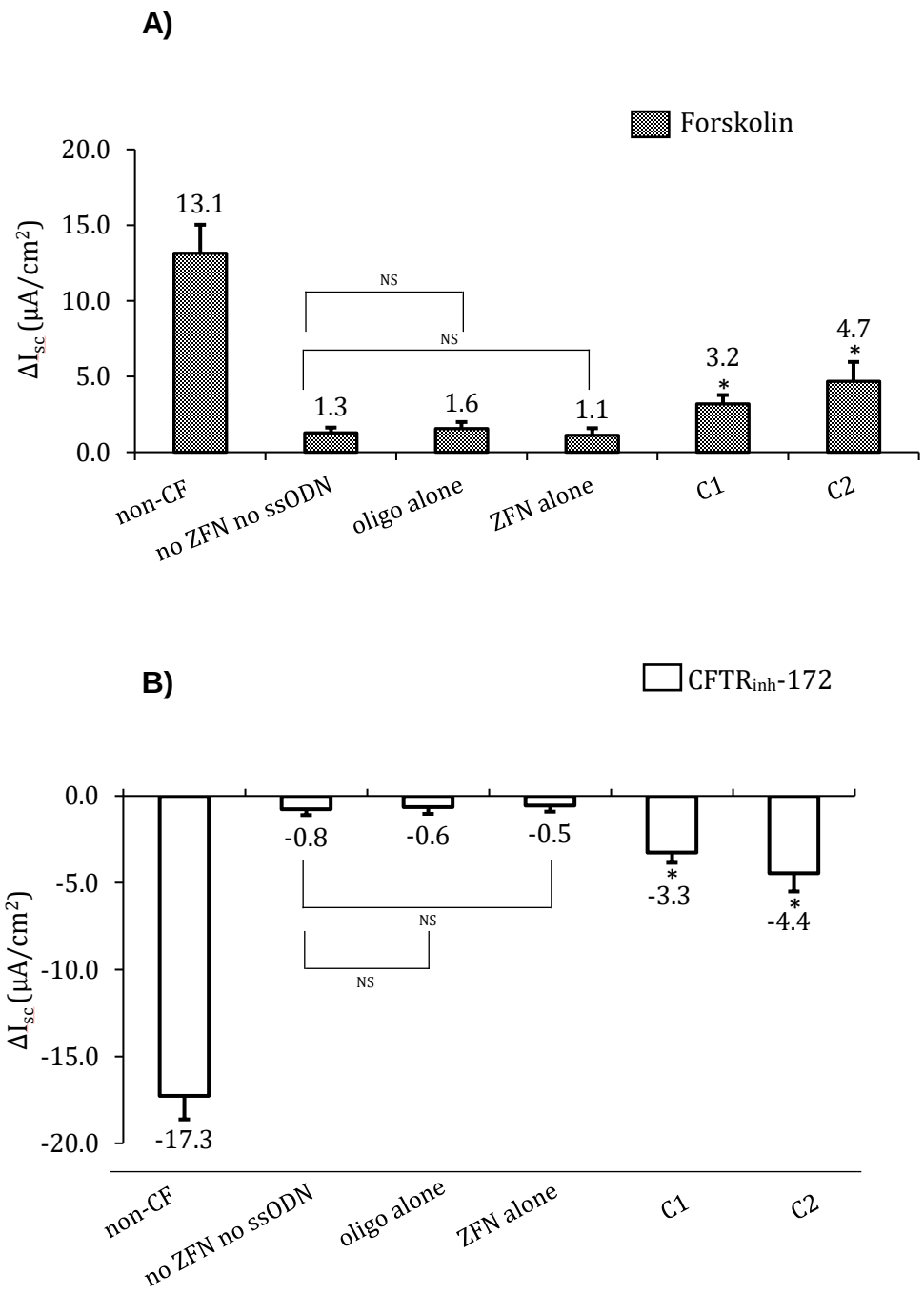
A)
Forskolin
20.0
15.0
10.0
5.0
0.0
ΔIsc (μA/cm2)
13.1
1.3
1.6
1.1
3.2
4.7
NS
NS
*
*
non-CF
no ZFN no ssODN
oligo alone
ZFN alone
C1
C2
B)
CFTRinh-172
0.0
-5.0
-10.0
-15.0
-20.0
ΔIsc (μA/cm2)
-17.3
-0.8
-0.6
-0.5
-3.3
-4.4
NS
NS
*
*
non-CF
no ZFN no ssODN
oligo alone
ZFN alone
C1
C2

5 were ΔF508/ΔF508, and 1 (clone #2) was amplified neither in the AS-PCR conditions nor in the PCR conditions for Sanger sequencing (we predicted this may be due to the presence of a large INDEL, but it was not tested further). Although we were successful in obtaining only one clone exhibiting correction of the ΔF508 mutation, this result is consistent with and verification of site-specific gene correction.

3.6 Optimization of ZFN Cutting Efficiency in Basal Cells Cultured in Pneumacult™-Ex Plus Medium

Pneumacult™-Ex plus medium (referred here as 'P-ex plus medium' or 'P-ex plus') is a defined medium produced by Stemcell Technologies for the expansion of primary human airway epithelial cells. The manufacturer, in technical materials, provided evidence that primary airway basal cells expanded in P-ex plus medium have significant proliferative capacity and also retain CFTR function. This led our laboratory to compare the proliferative and CFTR activity of basal cells cultured in the P-ex plus medium versus dual SMAD inh medium. Dr. Shingo Suzuki of our laboratory showed that basal cells in P-ex plus medium had higher proliferative capacity at earlier passages (earlier than passage 8) compared to those cultured in dual SMAD inh medium (data not shown). Furthermore, cells cultured in P-ex plus followed by ALI differentiation and Ussing chamber analyses showed higher CFTR channel activity as a function of passage number, as compared to dual SMAD inh cells (data not shown).

Conclusions from the study described above led to switching the culture medium for basal cells from the dual SMAD inh medium (used in the experiments described thus far) to P-ex plus medium. One of the other major reasons to do so was the possibility

FIGURE 3.10 Clonal isolation experiment. A) *Image at 10x magnification showing a basal-cell clone (yellow arrowhead) co-cultured with irradiated fibroblasts (seen surrounding the clone)* ***B)*** *Shown in purple is the forward primer for the AS-PCR we performed, reverse primer specific to* CFTR *WT sequence is shown in blue, and the reverse primer specific to the ΔF508 sequence is shown in green. The red triangle depicts ΔF508.* ***C)*** *15 clones were screened using AS-PCR, each with a primer pair specific to the wild-type allele and a primer pair specific to the mutant allele. The expected amplicon sizes were 392 and 389 bp, respectively. Clone #2 was not amplified in these PCR conditions. Wt/wt and mutant/mutant controls were used. Based on this screening test, clones # 5, 13, 19, 27 and 60 (**) were thought to give possible evidence for at least one wild-type allele.*

A)

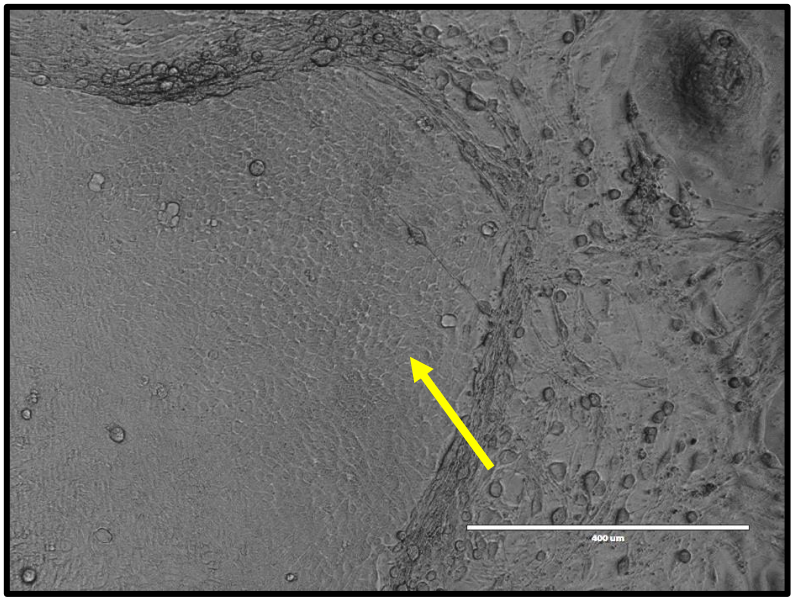
400 um

B)

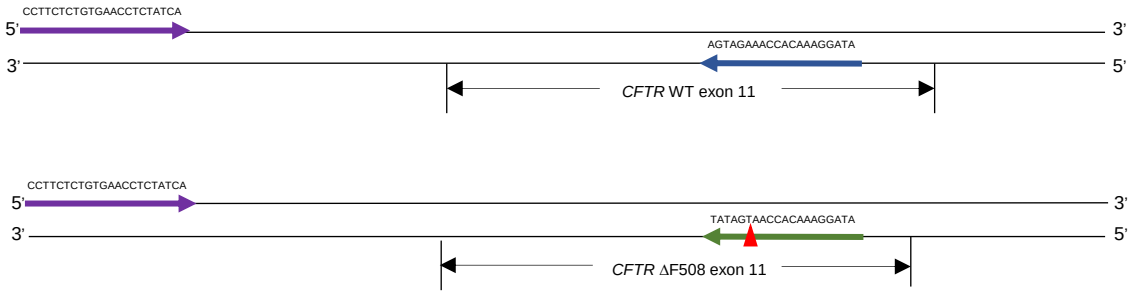
CCTTCTCTGTGAACCTCTATCA
5'
3'
AGTAGAAACCACAAAGGATA
3'
5'
CFTR WT exon 11
CCTTCTCTGTGAACCTCTATCA
5'
3'
TATAGTAACCACAAAGGATA
3'
5'
CFTR ΔF508 exon 11

C)

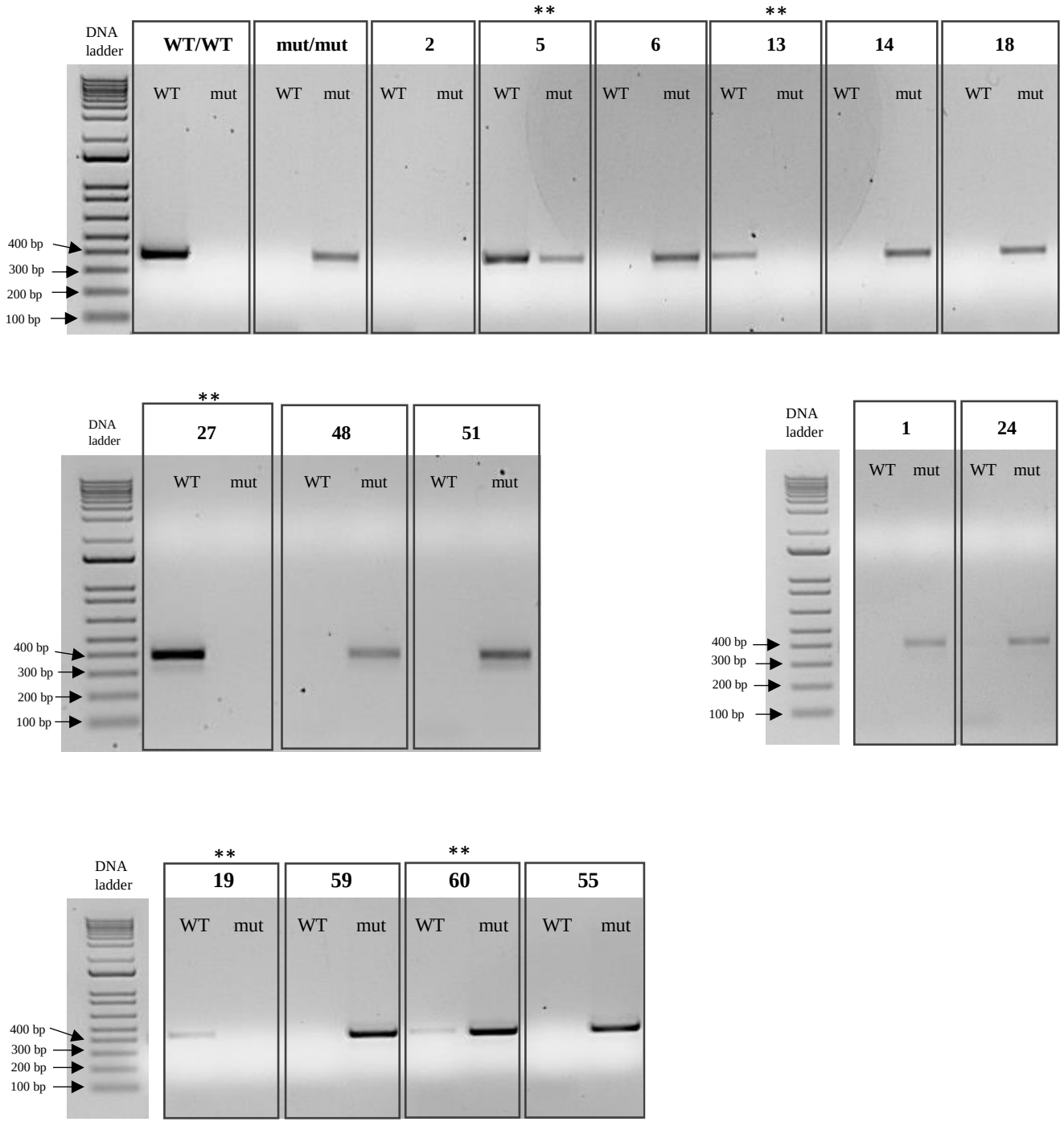
DNA ladder
WT/WT
mut/mut
2
5
6
13
14
18
**
**
WT
mut
400 bp
300 bp
200 bp
100 bp
DNA ladder
27
48
51
**
1
24
19
59
60
55

FIGURE 3.11 Clonal isolation experiment: Sanger sequencing analysis. A) *Clones #5, 13, 19, and 60, although shown to possibly have at least one wild-type allele by the AS-PCR, upon sequencing were found to be INDEL/mutant, INDEL/INDEL, INDEL/INDEL and mutant/mutant, respectively. Clone #27 was confirmed to have one allele with wild-type sequence. This was confirmation of site-specific gene correction.*

A)

CLONE #	***Allele1/Allele2***
27	WT/INDEL
13	INDEL/ INDEL
6	INDEL / INDEL
18	INDEL / INDEL
19	INDEL / INDEL
59	INDEL / INDEL
5	INDEL /ΔF508
55	INDEL /ΔF508
14	INDEL /ΔF508
1	ΔF508/ΔF508
48	ΔF508/ΔF508
51	ΔF508/ΔF508
24	ΔF508/ΔF508
60	ΔF508/ΔF508

that P-ex plus-cultured basal cells corrected at an early passage could perhaps retain their proliferative abilities through clonal isolation (as opposed to the senescence we observed) and subsequent expansion for further studies.

We tested the % cutting efficiency of ZFN + WPRE mRNA in P-ex plus-cultured basal cells. Three identical and independent experiments were conducted. The % NHEJ three days post-electroporation was assessed using TIDER analysis (FIGURE 3.12a). TIDER is a bioinformatics tool which quantifies % NHEJ and % gene correction using Sanger sequence trace decomposition. The total cell number, calculated three days post-electroporation for all three experiments, provided information regarding the cytotoxicity resulting from electroporation and/or ZFN cutting (FIGURE 3.12b). Based on % cutting efficiency and the observation that 4 and 8 µg of each ZFN resulted in greater cytotoxicity, we chose 2 µg each ZFN for optimization of gene correction conditions.

3.7 Optimization of Gene Correction in Basal Cells Cultured in Pneumacult™-Ex Plus medium

We conducted three identical and independent experiments in which 10, 20 and 30 µg of the 200-mer ssODN was transfected along with 2 µg each ZFN mRNA. The % NHEJ and % gene correction three days post-electroporation was assessed by TIDER analysis (FIGURE 3.13a). Cell number at this time point was calculated as a measure of cytotoxicity (FIGURE 3.13b). In these optimization experiments, the condition in which 2 µg each ZFN + 20 µg ssODN were transfected resulted in good frequency of correction with acceptable losses in cell number post transfection. Therefore, we decided to test this gene correction condition for CFTR functional restoration (FIGURE 3.13c).

Gene-corrected basal cells from experiments 1, 2 and 3 (FIGURE 3.13c) were subjected to *in vitro* differentiation using the ALI system. To visualize pseudostratified epithelium in the differentiated gene-corrected cells, hematoxylin and eosin staining (H&E staining) was done (FIGURE 3.14). We could observe pseudostratification in the corrected cells similar to that observed in the non-CF and ΔF508/ΔF508 controls.

Immunofluorescence studies using airway epithelial cell type-specific markers were performed on the differentiated gene-corrected cells. p63 and CK5 staining were used to visualize basal cells, MUC5AC staining for secretory cells, ACT (acetylated-tubulin) staining for ciliated cells, and FOXJ1 & FOXI1 staining to visualize ciliated cells and ionocytes, respectively (FIGURE 3.15). Comparing the relative quantification of each cell type (basal, secretory, ciliated and ionocytes) between the corrected cells and the wild-type and mutant controls provided information regarding the effect of genetic manipulation on the differentiation capacity of the corrected basal cells (FIGURE 3.16). In total, the H&E staining and immunostaining studies show that the *in vitro* differentiation abilities of the corrected basal cells were not observably affected by the gene editing manipulation.

FIGURE 3.12 ZFN dose response in basal cells cultured in P-ex plus medium: A) *% NHEJ as assessed by TIDER analysis. 0.5, 1, 2, 4 and 8 µg of each ZFN were tested for their cutting efficiency in three independent and identical experiments. Genomic DNA was analyzed three days post transfection. Genomic DNA from cells transfected with 1 µg GFP mRNA was used as a negative control. Mean values ± SD are presented* ***B)*** *Total cell number three days post-transfection were counted from three independent experiments. Mean values ± SD are presented.*

A)

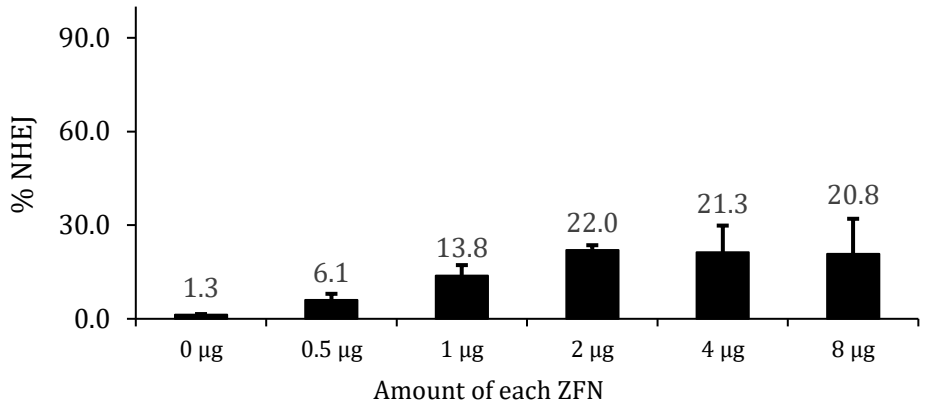
90.0
60.0
30.0
0.0
% NHEJ
1.3
6.1
13.8
22.0
21.3
20.8
0 µg
0.5 µg
1 µg
2 µg
4 µg
8 µg
Amount of each ZFN

B)

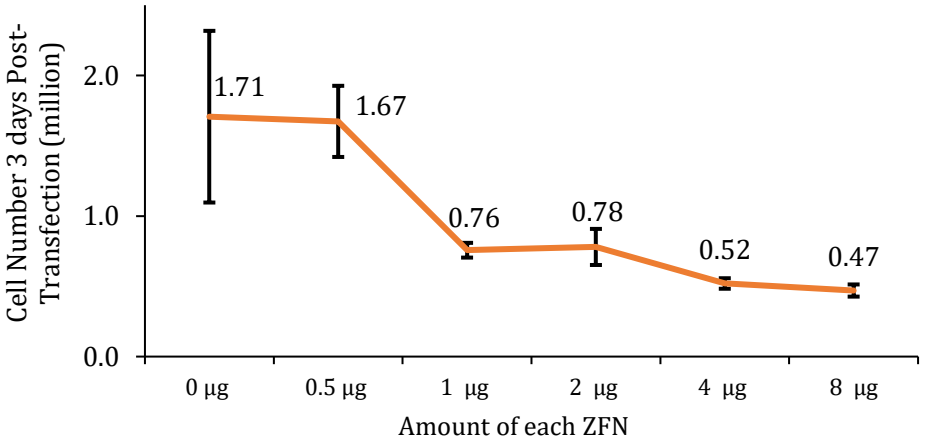
2.0
1.0
0.0
Cell Number 3 days Post-Transfection (million)
1.71
1.67
0.76
0.78
0.52
0.47
0 µg
0.5 µg
1 µg
2 µg
4 µg
8 µg
Amount of each ZFN

FIGURE 3.13 Gene correction of* CFTR *ΔF508/ΔF508 basal cells cultured in P-ex plus medium. A) *% NHEJ and % gene correction obtained by TIDER analysis is shown in the graph. 2 µg of each ZFN mRNA were transfected with 10, 20 and 30 µg of the 200-mer ssODN; genomic DNA was analyzed three days post transfection. This experiment was done in triplicate. DNA from cells transfected with 1 µg GFP mRNA was used as a negative control. Data are presented as mean ± SD.* ***B)*** *Total cell number was counted three days post-transfection for each of the three independent experiments in which 2 µg of each ZFN mRNA were transfected with 20 µg of the ssODN. Mean values ± SD are presented.* ***C)*** *Expt 1, expt 2, and expt 3 represent results from three independent experiments. These three samples were chosen for further studies.*

A)

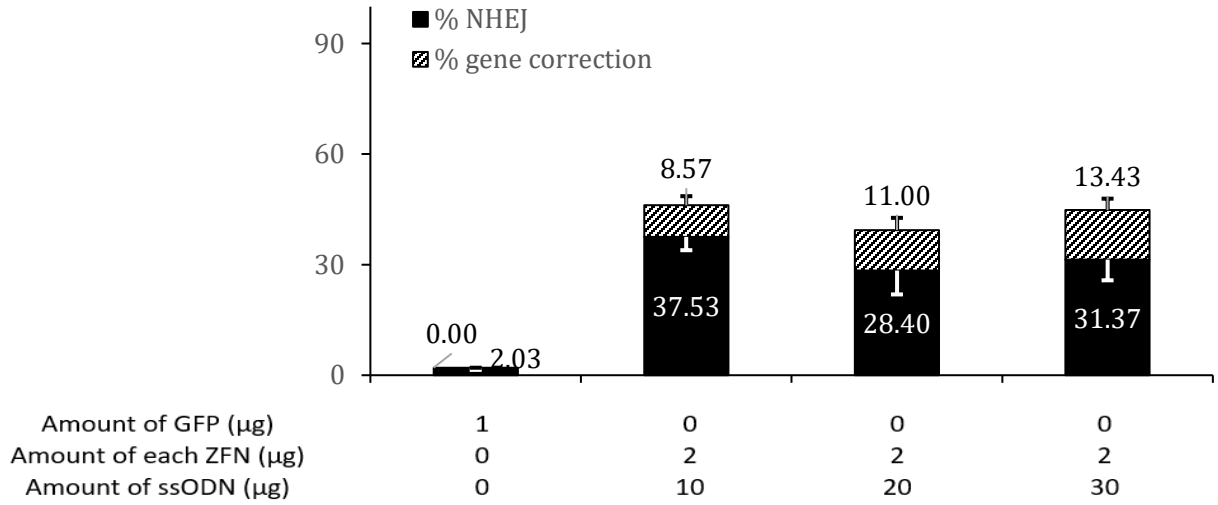
% NHEJ
% gene correction
90
60
30
0
0.00
2.03
8.57
37.53
11.00
28.40
13.43
31.37
Amount of GFP (µg) 1 0 0 0
Amount of each ZFN (µg) 0 2 2 2
Amount of ssODN (µg) 0 10 20 30

B)

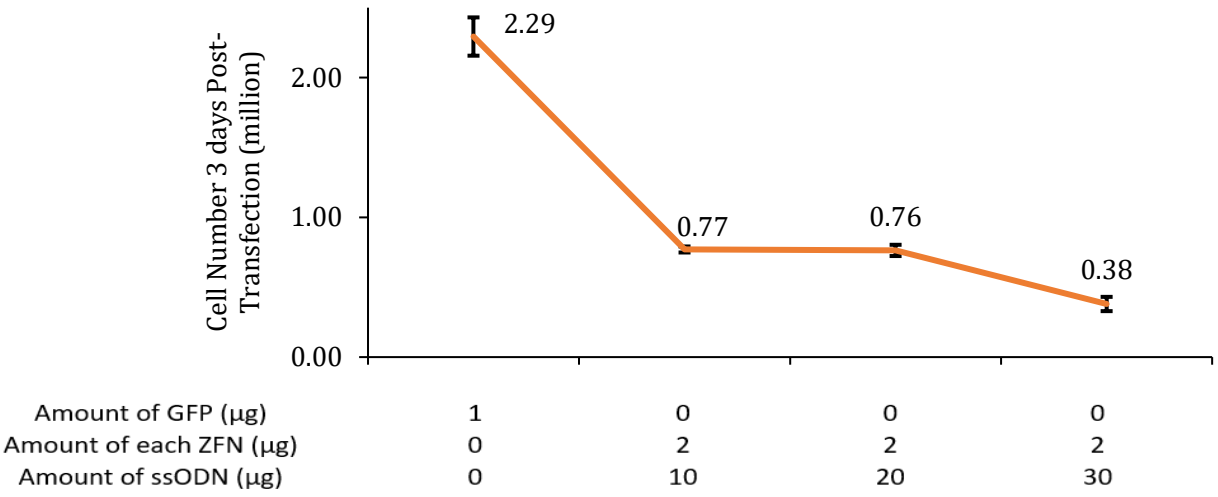
Cell Number 3 days Post-Transfection (million)
2.00
1.00
0.00
2.29
0.77
0.76
0.38
Amount of GFP (µg) 1 0 0 0
Amount of each ZFN (µg) 0 2 2 2
Amount of ssODN (µg) 0 10 20 30

C)

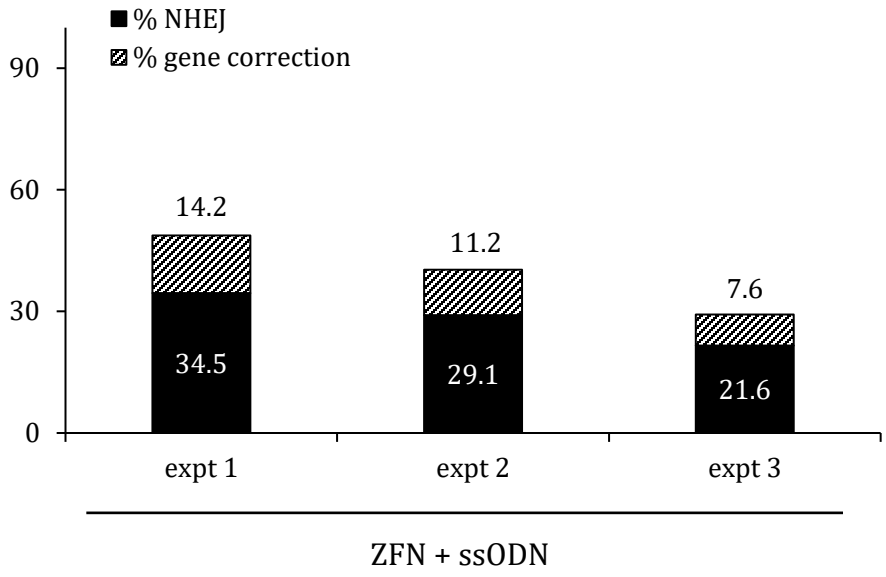
% NHEJ
% gene correction
90
60
30
0
14.2
11.2
7.6
34.5
29.1
21.6
expt 1
expt 2
expt 3
ZFN + ssODN

3.8 Demonstration of CFTR Protein Expression and Channel Activity in Gene-Corrected Cells

In the non-CF control, the mature fully-glycosylated CFTR protein was detected (~170 kDA) along with the core-glycosylated immature form (~140 kDa) whereas in the ΔF508/ΔF508 control sample, only the core-glycosylated CFTR was detected. This was as expected since ΔF508 homozygous cells do not produce mature CFTR. Most importantly, we detected the presence of fully-glycosylated CFTR protein (as well as the core-glycosylated form) in the corrected *in vitro* differentiated-cells (FIGURE 3.17).

By Ussing chamber analyses, we then assessed CFTR ion channel function (FIGURE 3.18). After baseline establishment by amiloride treatment, addition of cAMP-specific CFTR activator forskolin resulted in increased short-circuit current in the three differentiated gene-corrected samples. The ΔI_{sc} values were 8.9, 9.9 and 6.0 μA/cm^2, respectively. Importantly, these values were greater than that obtained in the ΔF508 homozygous mutant control ($p < 0.05$). Furthermore, the use of VX809 + VX770 (the components of Orkambi®), an FDA-approved combination drug shown to provide some therapeutic benefit to homozygous ΔF508 patients, allowed the comparison of ΔI_{sc} values obtained in the corrected cells with an accepted therapeutic range. Although our corrected samples yielded higher ΔI_{sc} values than uncorrected ΔF508/ΔF508, they did not rise to the level of VX809 + VX770-treated samples. Collectively, these data are evidence that the gene correction strategy in CF airway basal cells resulted in some restoration of CFTR protein expression and ion channel activity, albeit not yet in a therapeutic range.

FIGURE 3.14 H&E staining of ALI-cultured cells: *Histology studies were done on the ALI-differentiated cells. ZFN + ssODN expt 1, 2 and 3represent edited samples from three independent repeat experiments. Representative images are shown at 20X magnification.*

Non-CF

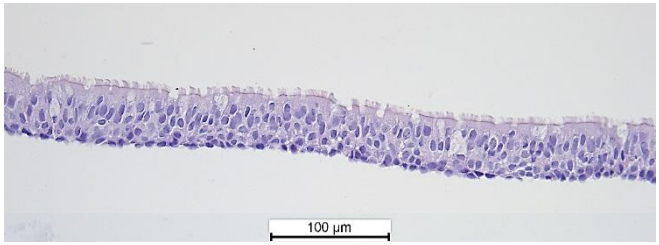

ΔF508/ΔF508

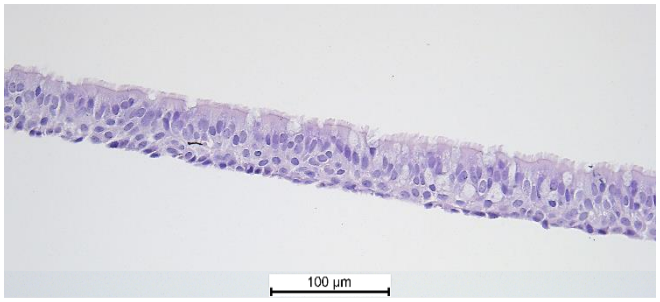

ZFN + ssODN expt 1

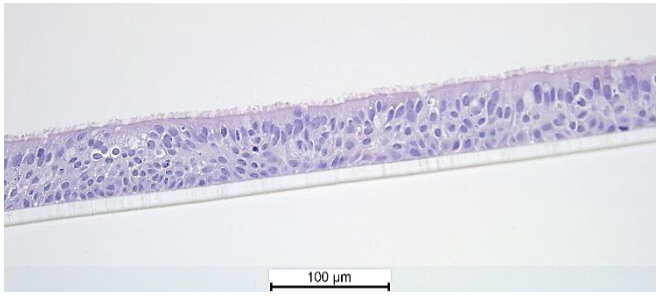

ZFN + ssODN expt 2

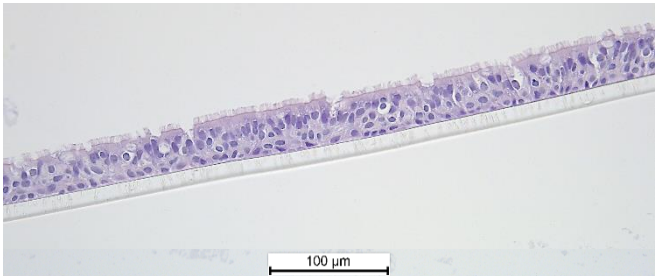

ZFN + ssODN expt 3

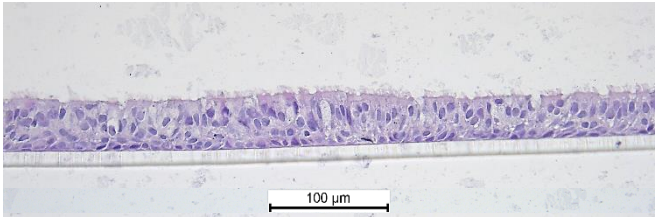

FIGURE 3.15 Immunofluorescence studies* of ALI-cultured cells:** *Representative images are shown at 40X magnification.* ***A) *CK5 (red) and ACT (green) staining basal cells and cilia, respectively.* ***B)*** *MUC5AC (red) and p63 (green) that stain secretory cells and basal cels, respectively.* ***C)*** *FOXJ1 (green) and FOXI1 (red) staining ciliated cell nuclei and ionocytes, respectively. Nuclei were counter-stained with 4,6'-diamidino-2-phenylindole (DAPI) (blue).*

A)

ACT CK5 DAPI

Non-CF

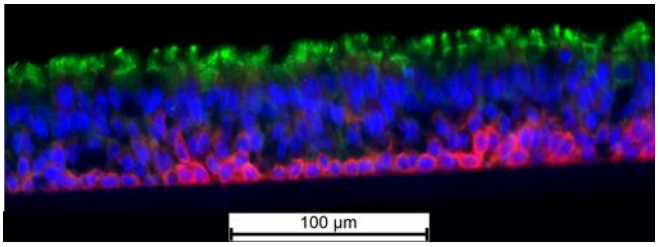

ΔF508/ΔF508

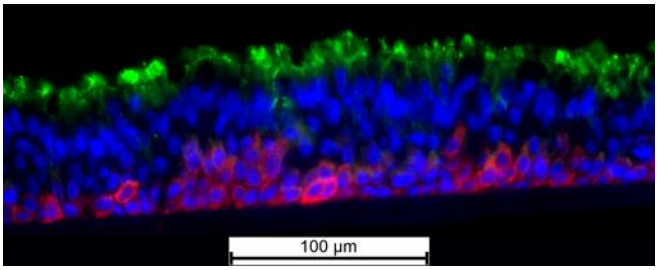

ZFN + ssODN expt 1

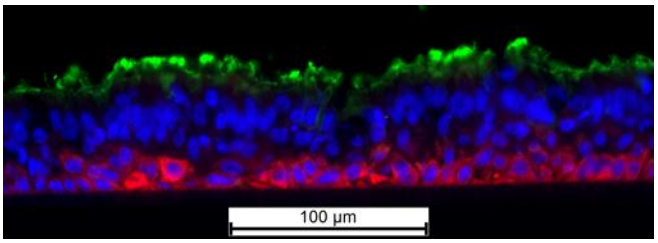

ZFN + ssODN expt 2

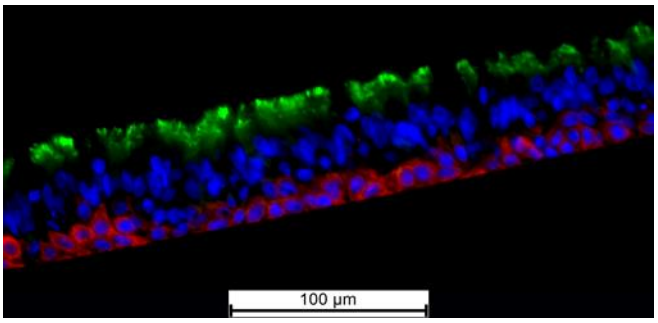

ZFN + ssODN expt 3

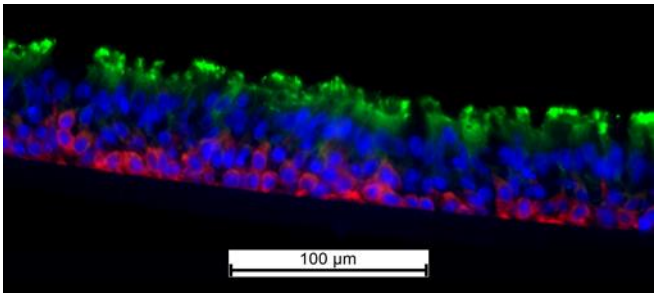

B)

p63 MUC5AC DAPI

Non-CF

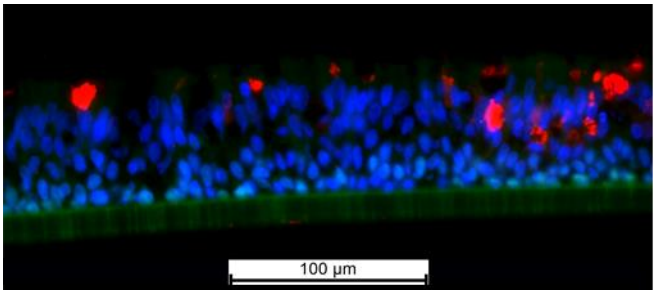

ΔF508/ΔF508

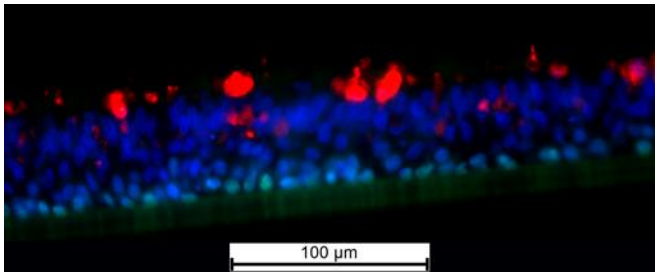

ZFN + ssODN expt 1

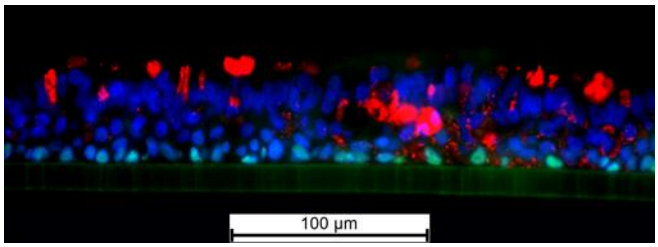

ZFN + ssODN expt 2

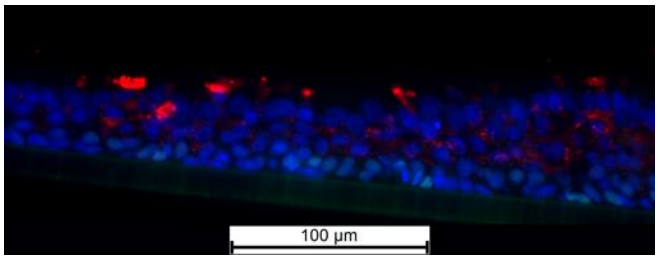

ZFN + ssODN expt 3

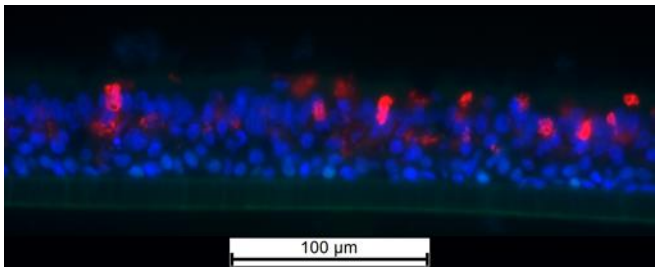

C)

FOXJ1 FOXI1 DAPI

Non-CF

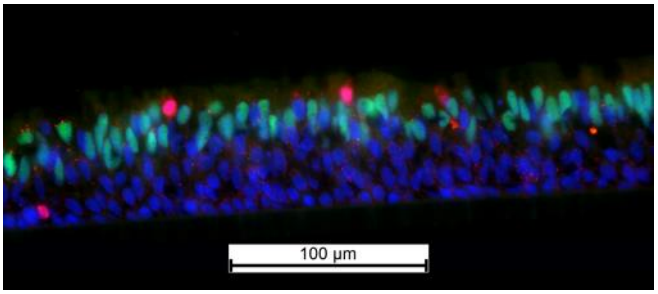

ΔF508/ΔF508

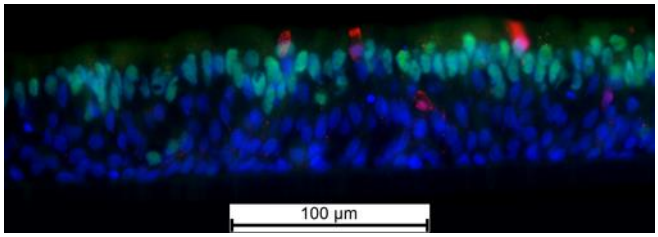

ZFN + ssODN expt 1

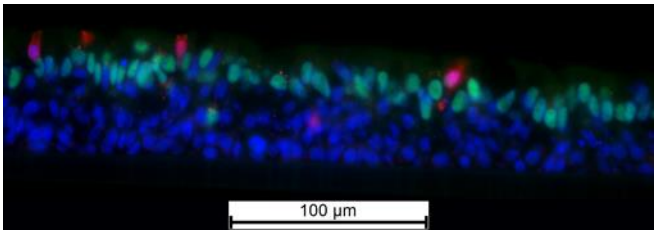

ZFN + ssODN expt 2

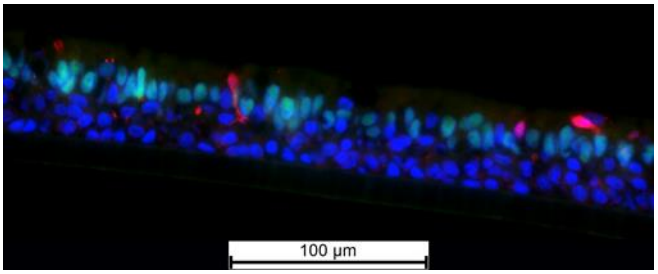

ZFN + ssODN expt 3

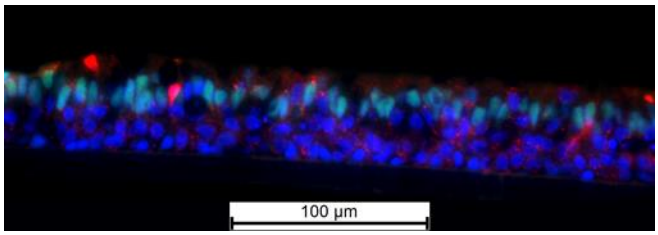

FIGURE 3.16 Relative quantification of airway epithelial cell-types. *Followed by immunofluorescence staining with markers specific to the cell types, images of 3 random fields (n=3) at 40x magnification were acquired. For a particular staining, in each of the 3 fields, cell number was counted relative to the total cell number (depicted by DAPI staining). Relative quantitation of basal cells* ***(A)****, secretory cells* ***(B)****, ciliated cells* ***(C)*** *and ionocytes* ***(D)*** *were done. Data are presented as mean ± SD.*

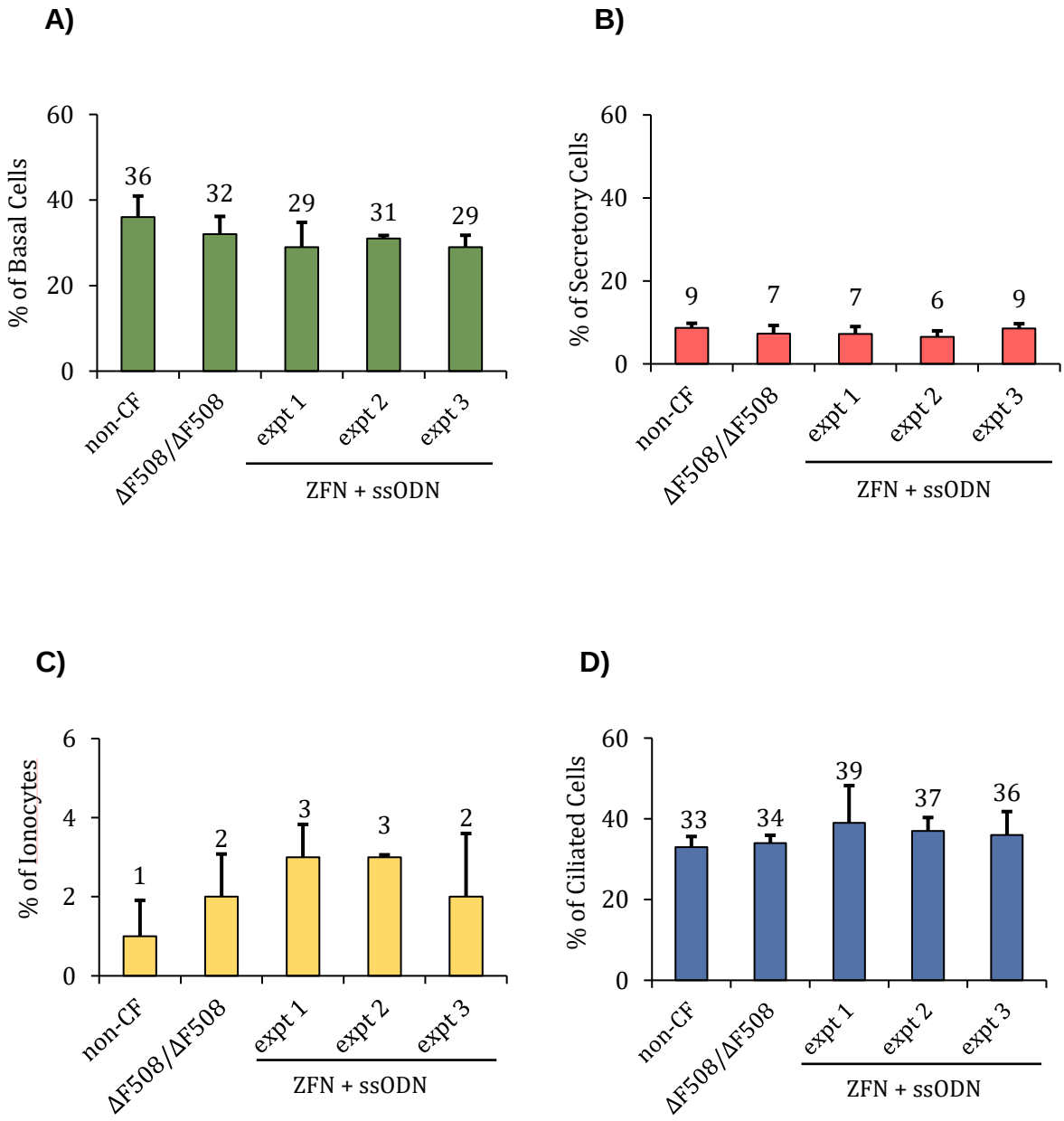
A)
% of Basal Cells
60
40
20
0
36
32
29
31
29
non-CF
ΔF508/ΔF508
expt 1
expt 2
expt 3
ZFN + ssODN
B)
% of Secretory Cells
60
40
20
0
9
7
7
6
9
non-CF
ΔF508/ΔF508
expt 1
expt 2
expt 3
ZFN + ssODN
C)
% of Ionocytes
6
4
2
0
1
2
3
3
2
non-CF
ΔF508/ΔF508
expt 1
expt 2
expt 3
ZFN + ssODN
D)
% of Ciliated Cells
60
40
20
0
33
34
39
37
36
non-CF
ΔF508/ΔF508
expt 1
expt 2
expt 3
ZFN + ssODN

FIGURE 3.17 Western blot analysis of restored CFTR protein. *Gene corrected cells (ZFN + ssODN expt 1, ZFN + ssODN expt 2, ZFN + ssODN expt 3) showed the presence of mature fully-glycosylated (~170 kDa) and immature core-glycosylated (~140 kDa) CFTR protein in contrast to the ΔF508/ΔF508 control in which only core-glycosylated protein was present. This demonstrates restored CFTR protein in gene-corrected cells. Non-CF cells showing presence of mature and immature CFTR was used as a positive control.*

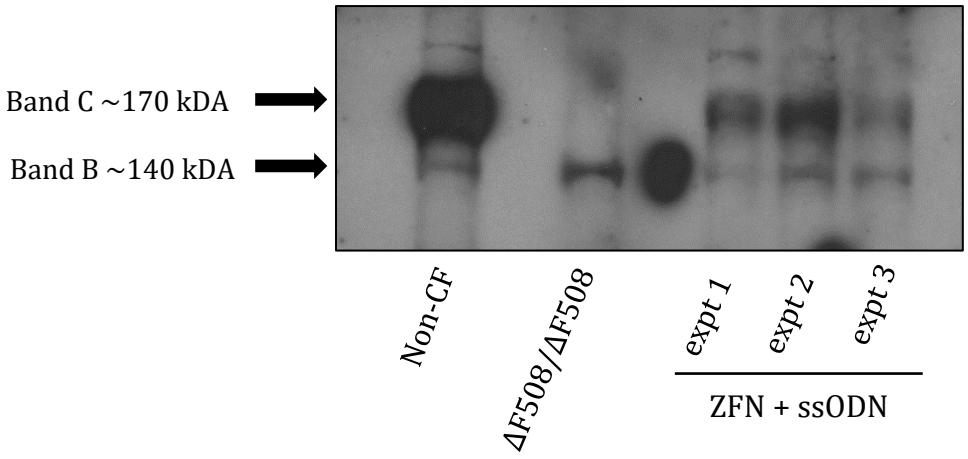

FIGURE 3.18 Ussing chamber analysis of ALI-cultured cells: *After 4 weeks of ALI differentiation, Ussing chamber analysis of CFTR function was performed. Negative control included ΔF508/ΔF508 cells. Non-CF cells were used as a positive control. All controls were at the same passage and were differentiated at the same time as the test samples. Each of the values obtained upon the action of forskolin and CFTR inh-172 in the three test samples were found to be greater than that in the negative control ($p < 0.05$). ΔF508/ΔF508 cells treated with VX809 + VX770 post-ALI differentiation and prior to electrophysiology studies served as a means of comparing ΔI_{sc} values obtained in the corrected cells with a therapeutic range. Data are presented as mean ± SD, 4 membrane inserts for each condition were analyzed (n=4).*

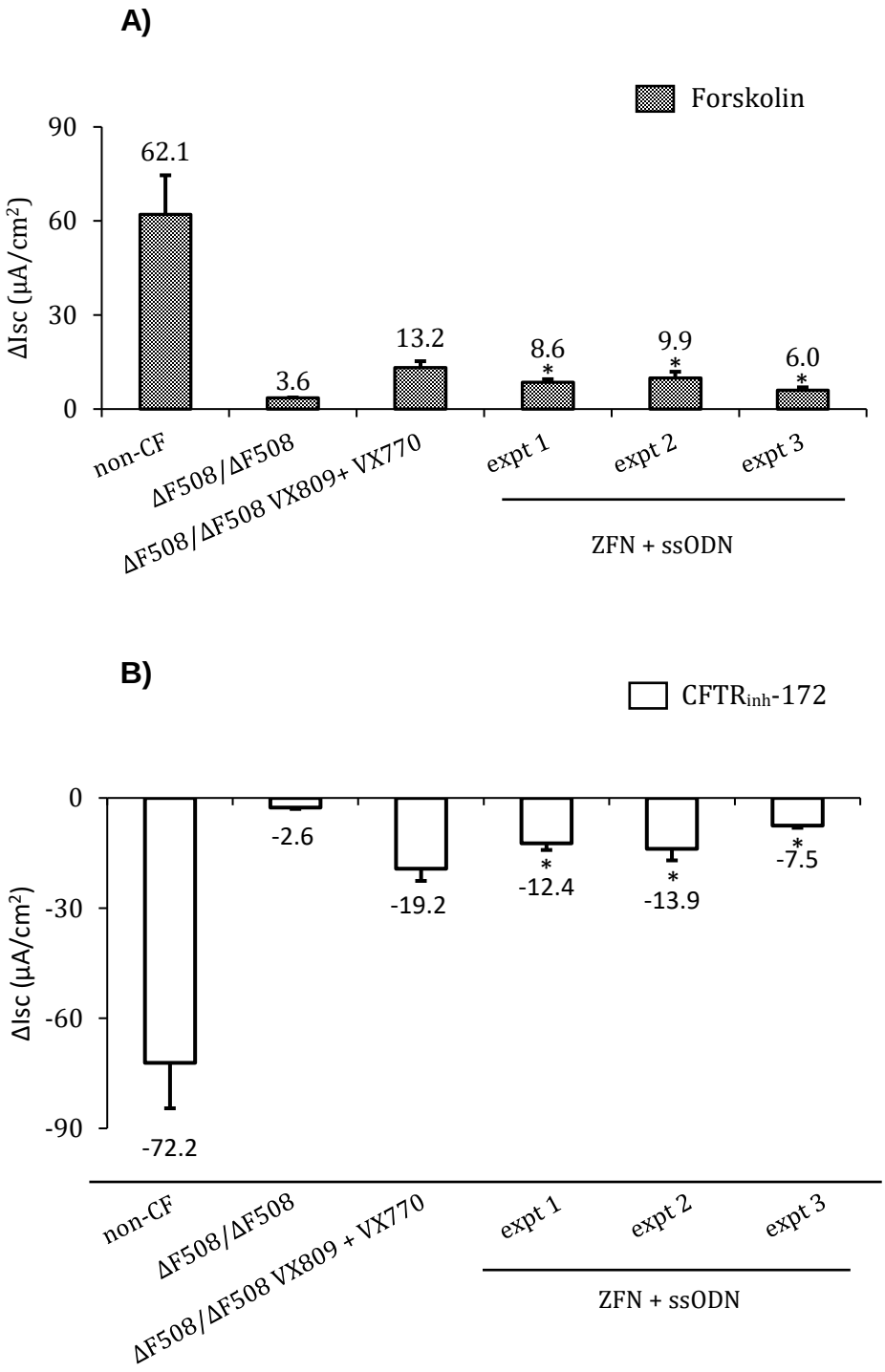
A)
Forskolin
90
60
30
0
ΔIsc (μA/cm²)
62.1
3.6
13.2
8.6
9.9
6.0
*
*
*
non-CF
ΔF508/ΔF508
ΔF508/ΔF508 VX809+ VX770
expt 1
expt 2
expt 3
ZFN + ssODN
B)
CFTRinh-172
0
-30
-60
-90
ΔIsc (μA/cm²)
-2.6
-19.2
-12.4
-13.9
-7.5
-72.2
*
*
*
non-CF
ΔF508/ΔF508
ΔF508/ΔF508 VX809 + VX770
expt 1
expt 2
expt 3
ZFN + ssODN

CHAPTER 4: DISCUSSION & FUTURE DIRECTIONS

In this study, we aimed to achieve *ex vivo* genetic correction of the most common *CFTR* mutation ΔF508 in airway basal cells utilizing engineered zinc-finger nucleases and single-stranded oligo donor DNA to facilitate gene editing. We specifically focused on airway basal cells due to their critical role in maintaining the respiratory epithelium.

In a study of DNA double-stranded break-induced gene targeting, it was shown that 80% of gene-targeting events occurred within 45 bp from the DSB (*74*). Indeed, research groups have reported efficient ZFN-induced gene editing at or within a few bp from the DSB (*30, 31, 75*). In our study, we used ΔF508-specific ZFNs which cut DNA ~8 bp from the ΔF508 mutation which we wish to restore to wild-type sequence (FIGURE 3.2). We first assessed the efficiency of the ZFNs, delivered in the form of mRNA via electroporation, to cause DSB in ΔF508/ΔF508 airway basal cells. The advantages of delivering ZFN as mRNA as opposed to plasmid DNA are fourfold: 1) lower cytotoxicity due to smaller size of RNA, 2) risk of random genome integration is eliminated, 3) short half-life of RNA lowers the probability of off-target events, and 4) higher cutting efficiency (*26*). We found that the addition of WPRE in the 3' UTR of ZFN mRNA enhanced % NHEJ ~4 to 12-fold (FIGURE 3.3c), in accordance with previously reported findings (*71*). Consistent INDEL rates were obtained between experiments using commercially-produced ZFN mRNA targeting *CFTR* ΔF508, and they were found to be dose-dependent; 25 to 70% NHEJ was achieved, depending on ZFN amount (FIGURE 3.5).

Donor DNA carrying the correcting sequence is required to facilitate gene correction; the length of homology arms is a crucial factor in determining its success rate. Using

ZFNs and a donor plasmid or ssODN, several groups had achieved pre-defined genomic modifications (*26, 30, 31)*. Using site-specific ZFNs, Chen *et al.* studied the efficacies of a 95-mer ssODN to insert a restriction site in the *AAVSI* locus in 7 different cell types (*26*). They showed that the ssODN efficiency was cell-type dependent (a range of 7 to 57 % insertion rates obtained), and also that the gene modification obtained using ssODN was ~two-fold higher than that obtained using a plasmid donor. It was reported by George Church *et al.* (2014) that having the desired mutation at the center of the ssODN, preferentially 70-130 bases in length, yielded efficient editing (*75*). Therefore, for ΔF508 gene correction, we aimed to optimize gene correction conditions in CF basal cells using ZFNs and a 100- or 200-mer ssODN; in both cases, the desired correcting sequence (insertion of CTT) was at the mid-point (FIGURE 3.6A). The 200-mer ssODN was found to be more efficient, yielding gene correction rates of ~8-10 % with 200-400 million copies per cell and thus, was used in our subsequent experiments (FIGURE 3.6b). We note that a 10% correction frequency per *CFTR* allele would imply that between 10 and 20% of cells were corrected depending on whether one or two alleles were corrected per cell.

We achieved 15.3-17.5% correction with transfection of 4 µg of each ZFN mRNA and 20 µg of the 200-mer ssODN (2 X 10^8 copies/cell) (FIGURE 3.7b). Air-liquid interface system was used for *in vitro* differentiation of the corrected basal cells into airway luminal cells and the differentiated cells demonstrated partial restoration of CFTR channel activity in Ussing chamber assays (ΔI_{sc} values of 3.2 and 4.7 µA/cm^2 after forskolin treatment) (FIGURE 3.9).

We used the CRC technique, in which basal cells are co-cultured with NIH3T3 mouse fibroblasts along with the ROCK inhibitor Y-27362, to enable single-cell clonal isolation from bulk-corrected basal cells (FIGURE 3.10). Pure corrected clones would enable us to determine whether correction occurred at one or both alleles. For future therapeutic use, it is possible that transplantation of a pure clone would be safer since it could be carefully assayed prior to transplantation for unwanted off-target events. From our clonal isolation experiment, we obtained one clone having a single wild-type *CFTR* allele, out of the 15 clones (30 *CFTR* alleles) that were analyzed (FIGURE 3.11). Although at low frequency, this was confirmation of site-specific gene correction. The clone could not, however, be expanded for further studies due to, we hypothesize, senescence at high passage number. A vast majority of the clones we obtained were found to have an INDEL in at least one allele. The consequences of an insertion or deletion in the immediate vicinity of ΔF508 in exon 11 remains to be determined. This is an important issue to consider for *in vivo* editing since the presence of an INDEL in the place of ΔF508 in both alleles could render it insensitive/unresponsive to the CFTR triple-drug treatment if eventually utilized as a back-up therapy for the gene editing.

We aimed to further improve our gene correction conditions by editing basal cells at an earlier passage and by changing the culture medium to increase the proliferation rate and better retain CFTR activity with passage number. This change of culture medium required us to re-optimize the editing protocol. In the P-ex plus culture conditions, we found that the optimum amount of the gene correction reagents that yielded good correction efficiency with acceptable levels of cytotoxicity was 2 µg each ZFN mRNA and 20 µg of ssODN (FIGURE 3.13). In three independent repeat experiments using

these conditions, we obtained correction rates of 7.6-14.2 %. This range of corrected alleles imply that we obtained 7.6 to 28.4 % cells that where corrected. The edited cells, which is a mixture of corrected and ΔF508/ΔF508 (with or without INDELs), were ALI-differentiated and immunofluorescence studies, Western blot & Ussing chamber analyses were done.

Our reason for performing immunofluorescence studies on the corrected cells was to check for adverse consequences of gene editing manipulation on the stemness of the transfected basal cells. Our results, based on quantification of immuno-stained airway epithelial cell types (basal, secretory, ciliated, and ionocytes), demonstrated that the differentiation capacities of the manipulated cells were comparable to that of the non-corrected CF and the non-CF cells (FIGURE 3.16). This is an important assessment since CF therapy employing transplantation of edited cells into the airways will rely on the stem cell potential of the corrected airway basal cells to repopulate the airway and differentiate into luminal cells carrying corrected *CFTR*.

The ΔF508 CFTR protein is pre-maturely degraded in the endoplasmic reticulum and therefore only core-glycosylated CFTR protein can be detected in Western blot analysis. Indeed, this was the case in our analysis, where the ΔF508/ΔF508 cells showed presence of only the immature core-glycosylated CFTR protein (~140 kDa), whereas non-CF cells demonstrated presence of both mature fully-glycosylated (~170 kDa) and immature CFTR. The gene-edited samples synthesized mature CFTR protein, albeit not at the same levels as non-CF controls, as well as its immature form (FIGURE 3.17). This provided evidence for the ability of our gene correction method to restore fully-glycosylated CFTR protein.

Comparison of band intensities in the western blots at various exposure times gave a rough estimation of the total mature CFTR synthesized in the corrected cells (the three edited replicate samples had 11 – 20.4% of total mature protein as compared to non-CF cells, respectively). Since trafficking of the CFTR protein to the cellular apical surface of ciliated cells is necessary for its function, CFTR immunofluorescence studies could provide information regarding its localization in the corrected cells and the cell types in which the protein is predominantly present (i. e. ciliated cells versus ionocytes).

By Ussing chamber analysis, we then assessed CFTR ion channel function in the three edited differentiated samples. An increase in chloride current was observed in the gene-corrected triplicates when compared with uncorrected CF cells, with the respective ΔI_{sc} values upon forskolin treatment 6.0 – 9.9 $\mu A/cm^2$. However, these values were lower than those obtained in the non-CF control cells, or the CF cells treated with the VX809 + VX770 drug combination (FIGURE 3.18). These results, although encouraging, call for further advances (some discussed below) in our current gene editing strategy to achieve a therapeutically relevant gene editing approach for CF.

After DSB resulting from the action of nucleases such as ZFNs, the cell predominately utilizes the template-independent NHEJ repair pathway to repair the lesion. This can be true even in the presence of a donor DNA carrying homologous sequences. Thus, there has been some effort to shift the balance to HR-mediated repair by specifically inhibiting the NHEJ pathway. Upon inhibiting DNA ligase IV (which is required for NHEJ) using SCR7, Hu *et al*. demonstrated an increase (~two-fold) in Cas9 and ssODN-directed gene modification in human cancer cells (*76*). Inhibition of a component of the DSB repair system, 53BP1, which is believed to favor NHEJ over

HDR, showed an improvement in gene targeting with double-stranded DNA and ZFN by ~5.6-fold (*77*). Thus, small molecules and inhibitors such as SCR7 and i53 (inhibitor of 53BP1) have the potential to enhance gene correction rates and one of the future goals of our study could will be to incorporate them to see if they facilitate attaining higher editing rates.

Another possible avenue for improving ΔF508 editing efficiency would be the delivery of the 'correcting' donor template. Our current strategy of ssODNs is limited both by toxicity of the delivered nucleic acid as well as the limited size of the homology sequences. Both limitation could potentially be overcome by donor delivery via viral vectors such as adeno-associated virus (AAV). AAV is a single-stranded DNA parvovirus and certain serotypes have been shown to have a natural tropism for lung epithelium. AAVs can transduce both dividing and non-dividing cells and this is one of the major advantages of gene transfer using AAV vectors to the slow-proliferating airway epithelium (*77 - 82*). Ellis *et al.* (2013) surveyed *ex vivo/in vitro* transduction efficiencies of mammalian primary cells with 10 different AAV serotypes, and they demonstrated that AAV6 had the greatest ability to transduce a wide range of cell types (*84*). Efficient HR-driven genome editing in hematopoietic stem cells has been reported using ZFN mRNA and AAV6 donors. The relative timings of ZFN and AAV6 delivery are a crucial determinant of the efficiency of gene editing and it has been shown that AAV6 transduction immediately after ZFN electroporation yields most efficient correction rates (*87)*. An alternative approach to ssODN-mediated gene correction of *CFTR* ΔF508 could, therefore, be transducing AAV6 vectors as homologous donor templates after ZFN electroporation. This method of donor DNA delivery could reduce the cytotoxicity

we observed in our experiments that resulted from the delivery of ssODNs by electroporation. AAV6 vectors could potentially carry larger homology arms (they have a maximum genome packaging size of ~4.5 kb) with less toxic effects on the cells and this could enhance gene correction to a great extent.

CRISPR/Cas9 is emerging as a new powerful system of genome engineering, in which the Cas9 DNA nuclease is recruited by a sequence-specific guide RNA (gRNA) to its target sequence. After the gRNA binds its specific DNA target through sequence complementation, Cas9 induces DSB (*89*). Nelson *et al.* had demonstrated successful gene correction in a mouse model of Duchenne muscular dystrophy (a genetic disease resulting from deletions of one or more exons in the dystrophin gene) using the CRISPR/Cas9 system (*90*). CRISPR-Cas9 mediated correction of *CFTR* ΔF508 in iPSCs has been demonstrated by two groups (*91, 92*). Therefore, the CRISPR/Cas9 editing system can be an alternative strategy to the ZFN-mediated gene correction of *CFTR* ΔF508 mutation.

One major concern in general for nuclease-mediated genome editing is the possibility of off-target events in the genomic DNA. It will, therefore, be imperative to either perform whole-genome sequencing on clonal populations or bioinformatically-guided NGS on predicted off-target sites in order that the corrected cells may be clinically applicable.

Accomplishing *in vivo* CF gene editing would require successful delivery of the editing reagents in the context of mucous-clogged CF airways and also reducing/preventing host immune responses to gene therapy agents. Clinical translation of the approach advanced in this project could take two forms. In the first, one could attempt to directly

edit the airway basal cells *in vivo.* In the second, *ex vivo* edited airway basal cells (as performed in this study, either as a pool of corrected and uncorrected cells or as a clonal population of corrected cells) could be transplanted back into the lungs of the affected CF patients. This will require transient injury methods to prepare the lung to take up the delivered cells. Our achievement in correcting the *CFTR* ΔF508 mutation with demonstration of partial restoration of wild-type protein processing and ion channel activity substantiates that gene modification strategies to treat and/or cure CF is attainable. With several further improvements, the described correction strategy may have the potential to bring us closer to ultimately accomplishing a therapeutic gene editing approach for CF.

CHAPTER 5: BIBLIOGRAPHY

1. Mou H, Vinarsky V, Tata PR, Brazauskas K, Choi SH, Crooke AK, Zhang B, Solomon GM, Turner B, Bihler H, Harrington J, Lapey A, Channick C, Keyes C, Freund A, Artandi S, Mense M, Rowe S, Engelhardt JF, Hsu YC, Rajagopal J. Dual SMAD Signaling Inhibition Enables Long-Term Expansion of Diverse Epithelial Basal Cells. Cell Stem Cell 2016;19:217-31.

2. Sophia Antoniou CE. Cystic Fibrosis. In: Suveer Singh FC, ed. MedicineMay 2016: e9-e10, 265-328.

3. Koch C, Hoiby N. Pathogenesis of cystic fibrosis. Lancet 1993;341:1065-9.

4. Orenstein DM, Winnie GB, Altman H. Cystic fibrosis: a 2002 update. J Pediatr 2002;140:156-64.

5. Bronstein MN, Sokol RJ, Abman SH, Chatfield BA, Hammond KB, Hambidge KM, Stall CD, Accurso FJ. Pancreatic insufficiency, growth, and nutrition in infants identified by newborn screening as having cystic fibrosis. J Pediatr 1992;120:533-40.

6. Stern RC, Rothstein FC, Doershuk CF. Treatment and prognosis of symptomatic gallbladder disease in patients with cystic fibrosis. J Pediatr Gastroenterol Nutr 1986;5:35-40.

7. Lamothe SM, Zhang S. Chapter Five - Ubiquitination of Ion Channels and Transporters. Prog Mol Biol Transl Sci 2016;141:161-223.

8. Anderson DH. Cystic fibrosis of the pancreas and its relation to celiac disease: A clinical and pathologic study. Am J Dis Child August 1938:344-99.

9. Cystic Fibrosis Foundation Patient Registry: 2017 Annual Data Report. 2017.

10. David M. Orenstein ENP, Patricia A. Nixxon, Elizabeth A. Ross, Robert M. Kaplan. Quality of well-being before and after antibiotic treatment of pulmonary exacerbation in patients with cystic fibrosis. Chest November 1990;98:1081-4.

11. Condren ME, Bradshaw MD. Ivacaftor: a novel gene-based therapeutic approach for cystic fibrosis. J Pediatr Pharmacol Ther 2013;18:8-13.

12. Van Goor F, Hadida S, Grootenhuis PD, Burton B, Stack JH, Straley KS, Decker CJ, Miller M, McCartney J, Olson ER, Wine JJ, Frizzell RA, Ashlock M, Negulescu PA. Correction of the F508del-CFTR protein processing defect in vitro by the investigational drug VX-809. Proc Natl Acad Sci U S A 2011;108:18843-8.

13. Sala MA, Jain M. Tezacaftor for the treatment of cystic fibrosis. Expert Rev Respir Med 2018;12:725-32.

14. Ratjen F, Bell SC, Rowe SM, Goss CH, Quittner AL, Bush A. Cystic fibrosis. Nat Rev Dis Primers 2015;1:15010.

15. Wang F, Zeltwanger S, Hu S, Hwang TC. Deletion of phenylalanine 508 causes attenuated phosphorylation-dependent activation of CFTR chloride channels. J Physiol 2000;524 Pt 3:637-48.

16. Hart SL, Harrison PT. Genetic therapies for cystic fibrosis lung disease. Curr Opin Pharmacol 2017;34:119-24.

17. Hacein-Bey Abina S, Gaspar HB, Blondeau J, Caccavelli L, Charrier S, Buckland K, Picard C, Six E, Himoudi N, Gilmour K, McNicol AM, Hara H, Xu-Bayford J,

Rivat C, Touzot F, Mavilio F, Lim A, Treluyer JM, Heritier S, Lefrere F, Magalon J, Pengue-Koyi I, Honnet G, Blanche S, Sherman EA, Male F, Berry C, Malani N, Bushman FD, Fischer A, Thrasher AJ, Galy A, Cavazzana M. Outcomes following gene therapy in patients with severe Wiskott-Aldrich syndrome. JAMA 2015;313:1550-63.

18. Aiuti A, Biasco L, Scaramuzza S, Ferrua F, Cicalese MP, Baricordi C, Dionisio F, Calabria A, Giannelli S, Castiello MC, Bosticardo M, Evangelio C, Assanelli A, Casiraghi M, Di Nunzio S, Callegaro L, Benati C, Rizzardi P, Pellin D, Di Serio C, Schmidt M, Von Kalle C, Gardner J, Mehta N, Neduva V, Dow DJ, Galy A, Miniero R, Finocchi A, Metin A, Banerjee PP, Orange JS, Galimberti S, Valsecchi MG, Biffi A, Montini E, Villa A, Ciceri F, Roncarolo MG, Naldini L. Lentiviral hematopoietic stem cell gene therapy in patients with Wiskott-Aldrich syndrome. Science 2013;341:1233151.

19. Salima Hacein-Bey-Abina S-TP, H. Bobby Gaspar, Myrium Armant, Charles C. Berry, Stephane Blanche, Jack Bleesing, Johanna Blondeau, Helen de Boer, Karen F. Buckland, Laure Caccavelli, Guilhem Cros. A modified gamma-retrovirus vector for X-linked severe combined immundeficiency. The New England Journal of Medicine October 9, 2014:1407-17.

20. Cavazzana-Calvo M, Payen E, Negre O, Wang G, Hehir K, Fusil F, Down J, Denaro M, Brady T, Westerman K, Cavallesco R, Gillet-Legrand B, Caccavelli L, Sgarra R, Maouche-Chretien L, Bernaudin F, Girot R, Dorazio R, Mulder GJ, Polack A, Bank A, Soulier J, Larghero J, Kabbara N, Dalle B, Gourmel B, Socie G, Chretien S, Cartier N, Aubourg P, Fischer A, Cornetta K, Galacteros F,

Beuzard Y, Gluckman E, Bushman F, Hacein-Bey-Abina S, Leboulch P. Transfusion independence and HMGA2 activation after gene therapy of human beta-thalassaemia. Nature 2010;467:318-22.

21. Mandal PK, Ferreira LM, Collins R, Meissner TB, Boutwell CL, Friesen M, Vrbanac V, Garrison BS, Stortchevoi A, Bryder D, Musunuru K, Brand H, Tager AM, Allen TM, Talkowski ME, Rossi DJ, Cowan CA. Efficient ablation of genes in human hematopoietic stem and effector cells using CRISPR/Cas9. Cell Stem Cell 2014;15:643-52.

22. Wang M, Glass ZA, Xu Q. Non-viral delivery of genome-editing nucleases for gene therapy. Gene Ther 2017;24:144-50.

23. Rui Y, Wilson DR, Green JJ. Non-Viral Delivery To Enable Genome Editing. Trends Biotechnol 2018.

24. Carroll D. Genome engineering with zinc-finger nucleases. Genetics 2011;188:773-82.

25. Carroll D. Progress and prospects: zinc-finger nucleases as gene therapy agents. Gene Ther 2008;15:1463-8.

26. Chen F, Pruett-Miller SM, Huang Y, Gjoka M, Duda K, Taunton J, Collingwood TN, Frodin M, Davis GD. High-frequency genome editing using ssDNA oligonucleotides with zinc-finger nucleases. Nat Methods 2011;8:753-5.

27. Porteus MH. Mammalian gene targeting with designed zinc finger nucleases. Mol Ther 2006;13:438-46.

28. Santiago Y, Chan E, Liu PQ, Orlando S, Zhang L, Urnov FD, Holmes MC, Guschin D, Waite A, Miller JC, Rebar EJ, Gregory PD, Klug A, Collingwood TN. Targeted gene knockout in mammalian cells by using engineered zinc-finger nucleases. Proc Natl Acad Sci U S A 2008;105:5809-14.

29. Perez EE, Wang J, Miller JC, Jouvenot Y, Kim KA, Liu O, Wang N, Lee G, Bartsevich VV, Lee YL, Guschin DY, Rupniewski I, Waite AJ, Carpenito C, Carroll RG, Orange JS, Urnov FD, Rebar EJ, Ando D, Gregory PD, Riley JL, Holmes MC, June CH. Establishment of HIV-1 resistance in CD4+ T cells by genome editing using zinc-finger nucleases. Nat Biotechnol 2008;26:808-16.

30. Moehle EA, Rock JM, Lee YL, Jouvenot Y, DeKelver RC, Gregory PD, Urnov FD, Holmes MC. Targeted gene addition into a specified location in the human genome using designed zinc finger nucleases. Proc Natl Acad Sci U S A 2007;104:3055-60.

31. Urnov FD, Miller JC, Lee YL, Beausejour CM, Rock JM, Augustus S, Jamieson AC, Porteus MH, Gregory PD, Holmes MC. Highly efficient endogenous human gene correction using designed zinc-finger nucleases. Nature 2005;435:646-51.

32. Zou J, Maeder ML, Mali P, Pruett-Miller SM, Thibodeau-Beganny S, Chou BK, Chen G, Ye Z, Park IH, Daley GQ, Porteus MH, Joung JK, Cheng L. Gene targeting of a disease-related gene in human induced pluripotent stem and embryonic stem cells. Cell Stem Cell 2009;5:97-110.

33. Chandrasegaran S. Recent advances in the use of ZFN-mediated gene editing for human gene therapy. Cell Gene Ther Insights 2017;3:33-41.

34. Miller JC, Holmes MC, Wang J, Guschin DY, Lee YL, Rupniewski I, Beausejour CM, Waite AJ, Wang NS, Kim KA, Gregory PD, Pabo CO, Rebar EJ. An improved zinc-finger nuclease architecture for highly specific genome editing. Nat Biotechnol 2007;25:778-85.

35. Szczepek M, Brondani V, Buchel J, Serrano L, Segal DJ, Cathomen T. Structure-based redesign of the dimerization interface reduces the toxicity of zinc-finger nucleases. Nat Biotechnol 2007;25:786-93.

36. Ramalingam S, Kandavelou K, Rajenderan R, Chandrasegaran S. Creating designed zinc-finger nucleases with minimal cytotoxicity. J Mol Biol 2011;405:630-41.

37. Boers JE, Ambergen AW, Thunnissen FB. Number and proliferation of basal and parabasal cells in normal human airway epithelium. Am J Respir Crit Care Med 1998;157:2000-6.

38. Evans MJ, Van Winkle LS, Fanucchi MV, Plopper CG. Cellular and molecular characteristics of basal cells in airway epithelium. Exp Lung Res 2001;27:401-15.

39. Rock JR, Onaitis MW, Rawlins EL, Lu Y, Clark CP, Xue Y, Randell SH, Hogan BL. Basal cells as stem cells of the mouse trachea and human airway epithelium. Proc Natl Acad Sci U S A 2009;106:12771-5.

40. Rock JR, Randell SH, Hogan BL. Airway basal stem cells: a perspective on their roles in epithelial homeostasis and remodeling. Dis Model Mech 2010;3:545-56.

41. Hong KU, Reynolds SD, Watkins S, Fuchs E, Stripp BR. Basal cells are a multipotent progenitor capable of renewing the bronchial epithelium. Am J Pathol 2004;164:577-88.

42. Hackett TL, Shaheen F, Johnson A, Wadsworth S, Pechkovsky DV, Jacoby DB, Kicic A, Stick SM, Knight DA. Characterization of side population cells from human airway epithelium. Stem Cells 2008;26:2576-85.

43. Borthwick DW, Shahbazian M, Krantz QT, Dorin JR, Randell SH. Evidence for stem-cell niches in the tracheal epithelium. Am J Respir Cell Mol Biol 2001;24:662-70.

44. Hong KU, Reynolds SD, Watkins S, Fuchs E, Stripp BR. In vivo differentiation potential of tracheal basal cells: evidence for multipotent and unipotent subpopulations. Am J Physiol Lung Cell Mol Physiol 2004;286:L643-9.

45. Daniely Y, Liao G, Dixon D, Linnoila RI, Lori A, Randell SH, Oren M, Jetten AM. Critical role of p63 in the development of a normal esophageal and tracheobronchial epithelium. Am J Physiol Cell Physiol 2004;287:C171-81.

46. Hajj R, Baranek T, Le Naour R, Lesimple P, Puchelle E, Coraux C. Basal cells of the human adult airway surface epithelium retain transit-amplifying cell properties. Stem Cells 2007;25:139-48.

47. Evans MJ, Moller PC. Biology of airway basal cells. Exp Lung Res 1991;17:513-31.

48. Avril-Delplanque A, Casal I, Castillon N, Hinnrasky J, Puchelle E, Peault B. Aquaporin-3 expression in human fetal airway epithelial progenitor cells. Stem Cells 2005;23:992-1001.

49. Butler CR, Hynds RE, Gowers KH, Lee Ddo H, Brown JM, Crowley C, Teixeira VH, Smith CM, Urbani L, Hamilton NJ, Thakrar RM, Booth HL, Birchall MA, De Coppi P, Giangreco A, O'Callaghan C, Janes SM. Rapid Expansion of Human Epithelial Stem Cells Suitable for Airway Tissue Engineering. Am J Respir Crit Care Med 2016;194:156-68.

50. Suprynowicz FA, Upadhyay G, Krawczyk E, Kramer SC, Hebert JD, Liu X, Yuan H, Cheluvaraju C, Clapp PW, Boucher RC, Jr., Kamonjoh CM, Randell SH, Schlegel R. Conditionally reprogrammed cells represent a stem-like state of adult epithelial cells. Proc Natl Acad Sci U S A 2012;109:20035-40.

51. Montoro DT, Haber AL, Biton M, Vinarsky V, Lin B, Birket SE, Yuan F, Chen S, Leung HM, Villoria J, Rogel N, Burgin G, Tsankov AM, Waghray A, Slyper M, Waldman J, Nguyen L, Dionne D, Rozenblatt-Rosen O, Tata PR, Mou H, Shivaraju M, Bihler H, Mense M, Tearney GJ, Rowe SM, Engelhardt JF, Regev A, Rajagopal J. A revised airway epithelial hierarchy includes CFTR-expressing ionocytes. Nature 2018;560:319-24.

52. Trapnell BC, Chu CS, Paakko PK, Banks TC, Yoshimura K, Ferrans VJ, Chernick MS, Crystal RG. Expression of the cystic fibrosis transmembrane conductance regulator gene in the respiratory tract of normal individuals and individuals with cystic fibrosis. Proc Natl Acad Sci U S A 1991;88:6565-9.

53. Engelhardt JF, Zepeda M, Cohn JA, Yankaskas JR, Wilson JM. Expression of the cystic fibrosis gene in adult human lung. J Clin Invest 1994;93:737-49.

54. Engelhardt JF, Yankaskas JR, Ernst SA, Yang Y, Marino CR, Boucher RC, Cohn JA, Wilson JM. Submucosal glands are the predominant site of CFTR expression in the human bronchus. Nat Genet 1992;2:240-8.

55. Kreda SM, Mall M, Mengos A, Rochelle L, Yankaskas J, Riordan JR, Boucher RC. Characterization of wild-type and deltaF508 cystic fibrosis transmembrane regulator in human respiratory epithelia. Mol Biol Cell 2005;16:2154-67.

56. Johnson LG, Olsen JC, Sarkadi B, Moore KL, Swanstrom R, Boucher RC. Efficiency of gene transfer for restoration of normal airway epithelial function in cystic fibrosis. Nat Genet 1992;2:21-5.

57. Farmen SL, Karp PH, Ng P, Palmer DJ, Koehler DR, Hu J, Beaudet AL, Zabner J, Welsh MJ. Gene transfer of CFTR to airway epithelia: low levels of expression are sufficient to correct Cl- transport and overexpression can generate basolateral CFTR. Am J Physiol Lung Cell Mol Physiol 2005;289:L1123-30.

58. Goldman MJ, Yang Y, Wilson JM. Gene therapy in a xenograft model of cystic fibrosis lung corrects chloride transport more effectively than the sodium defect. Nat Genet 1995;9:126-31.

59. Riordan JR, Rommens JM, Kerem B, Alon N, Rozmahel R, Grzelczak Z, Zielenski J, Lok S, Plavsic N, Chou JL. Identification of the cystic fibrosis gene: cloning and characterization of complementary DNA. Science 1989;245:1066-73.

60. Rommens JM, Iannuzzi MC, Kerem B, Drumm ML, Melmer G, Dean M, Rozmahel R, Cole JL, Kennedy D, Hidaka N. Identification of the cystic fibrosis gene: chromosome walking and jumping. Science 1989;245:1059-65.

61. Kerem B, Rommens JM, Buchanan JA, Markiewicz D, Cox TK, Chakravarti A, Buchwald M, Tsui LC. Identification of the cystic fibrosis gene: genetic analysis. Science 1989;245:1073-80.

62. Drumm ML, Pope HA, Cliff WH, Rommens JM, Marvin SA, Tsui LC, Collins FS, Frizzell RA, Wilson JM. Correction of the cystic fibrosis defect in vitro by retrovirus-mediated gene transfer. Cell 1990;62:1227-33.

63. Rich DP, Anderson MP, Gregory RJ, Cheng SH, Paul S, Jefferson DM, McCann JD, Klinger KW, Smith AE, Welsh MJ. Expression of cystic fibrosis transmembrane conductance regulator corrects defective chloride channel regulation in cystic fibrosis airway epithelial cells. Nature 1990;347:358-63.

64. Steines B, Dickey DD, Bergen J, Excoffon KJ, Weinstein JR, Li X, Yan Z, Abou Alaiwa MH, Shah VS, Bouzek DC, Powers LS, Gansemer ND, Ostedgaard LS, Engelhardt JF, Stoltz DA, Welsh MJ, Sinn PL, Schaffer DV, Zabner J. CFTR gene transfer with AAV improves early cystic fibrosis pig phenotypes. JCI Insight 2016;1:e88728.

65. Vidovic D, Carlon MS, da Cunha MF, Dekkers JF, Hollenhorst MI, Bijvelds MJ, Ramalho AS, Van den Haute C, Ferrante M, Baekelandt V, Janssens HM, De Boeck K, Sermet-Gaudelus I, de Jonge HR, Gijsbers R, Beekman JM, Edelman A, Debyser Z. rAAV-CFTRDeltaR Rescues the Cystic Fibrosis Phenotype in

Human Intestinal Organoids and Cystic Fibrosis Mice. Am J Respir Crit Care Med 2016;193:288-98.

66. Cooney AL, Abou Alaiwa MH, Shah VS, Bouzek DC, Stroik MR, Powers LS, Gansemer ND, Meyerholz DK, Welsh MJ, Stoltz DA, Sinn PL, McCray PB, Jr. Lentiviral-mediated phenotypic correction of cystic fibrosis pigs. JCI Insight 2016;1.

67. Alton EW, Beekman JM, Boyd AC, Brand J, Carlon MS, Connolly MM, Chan M, Conlon S, Davidson HE, Davies JC, Davies LA, Dekkers JF, Doherty A, Gea-Sorli S, Gill DR, Griesenbach U, Hasegawa M, Higgins TE, Hironaka T, Hyndman L, McLachlan G, Inoue M, Hyde SC, Innes JA, Maher TM, Moran C, Meng C, Paul-Smith MC, Pringle IA, Pytel KM, Rodriguez-Martinez A, Schmidt AC, Stevenson BJ, Sumner-Jones SG, Toshner R, Tsugumine S, Wasowicz MW, Zhu J. Preparation for a first-in-man lentivirus trial in patients with cystic fibrosis. Thorax 2017;72:137-47.

68. Lee CM, Flynn R, Hollywood JA, Scallan MF, Harrison PT. Correction of the DeltaF508 Mutation in the Cystic Fibrosis Transmembrane Conductance Regulator Gene by Zinc-Finger Nuclease Homology-Directed Repair. Biores Open Access 2012;1:99-108.

69. Crane AM, Kramer P, Bui JH, Chung WJ, Li XS, Gonzalez-Garay ML, Hawkins F, Liao W, Mora D, Choi S, Wang J, Sun HC, Paschon DE, Guschin DY, Gregory PD, Kotton DN, Holmes MC, Sorscher EJ, Davis BR. Targeted correction and

restored function of the CFTR gene in cystic fibrosis induced pluripotent stem cells. Stem Cell Reports 2015;4:569-77.

70. Hockemeyer D, Soldner F, Beard C, Gao Q, Mitalipova M, DeKelver RC, Katibah GE, Amora R, Boydston EA, Zeitler B, Meng X, Miller JC, Zhang L, Rebar EJ, Gregory PD, Urnov FD, Jaenisch R. Efficient targeting of expressed and silent genes in human ESCs and iPSCs using zinc-finger nucleases. Nat Biotechnol 2009;27:851-7.

71. Jessica M. Ong CRB, Matthew C. Mendel, and Gregory J. Cost. The WPRE improves genetic engineering with site-specific nucleases. 2017.

72. Reynolds SD, Rios C, Wesolowska-Andersen A, Zhuang Y, Pinter M, Happoldt C, Hill CL, Lallier SW, Cosgrove GP, Solomon GM, Nichols DP, Seibold MA. Airway Progenitor Clone Formation Is Enhanced by Y-27632-Dependent Changes in the Transcriptome. Am J Respir Cell Mol Biol 2016;55:323-36.

73. Elliott B, Richardson C, Winderbaum J, Nickoloff JA, Jasin M. Gene conversion tracts from double-strand break repair in mammalian cells. Mol Cell Biol 1998;18:93-101.

74. Maeder ML, Thibodeau-Beganny S, Sander JD, Voytas DF, Joung JK. Oligomerized pool engineering (OPEN): an 'open-source' protocol for making customized zinc-finger arrays. Nat Protoc 2009;4:1471-501.

75. Byrne SM, Mali P, Church GM. Genome editing in human stem cells. Methods Enzymol 2014;546:119-38.

76. Hu Z, Shi Z, Guo X, Jiang B, Wang G, Luo D, Chen Y, Zhu YS. Ligase IV inhibitor SCR7 enhances gene editing directed by CRISPR-Cas9 and ssODN in human cancer cells. Cell Biosci 2018;8:12.

77. MM Ayers PJ. Proliferation and differentiation in mammalian airway epithelium. European Respiratory Journal 1988.

78. Kessler PD, Podsakoff GM, Chen X, McQuiston SA, Colosi PC, Matelis LA, Kurtzman GJ, Byrne BJ. Gene delivery to skeletal muscle results in sustained expression and systemic delivery of a therapeutic protein. Proc Natl Acad Sci U S A 1996;93:14082-7.

79. Koeberl DD, Alexander IE, Halbert CL, Russell DW, Miller AD. Persistent expression of human clotting factor IX from mouse liver after intravenous injection of adeno-associated virus vectors. Proc Natl Acad Sci U S A 1997;94:1426-31.

80. Koeberl DD, Bonham L, Halbert CL, Allen JM, Birkebak T, Miller AD. Persistent, therapeutically relevant levels of human granulocyte colony-stimulating factor in mice after systemic delivery of adeno-associated virus vectors. Hum Gene Ther 1999;10:2133-40.

81. Muzyczka N. Use of adeno-associated virus as a general transduction vector for mammalian cells. Curr Top Microbiol Immunol 1992;158:97-129.

82. Snyder RO, Miao CH, Patijn GA, Spratt SK, Danos O, Nagy D, Gown AM, Winther B, Meuse L, Cohen LK, Thompson AR, Kay MA. Persistent and

therapeutic concentrations of human factor IX in mice after hepatic gene transfer of recombinant AAV vectors. Nat Genet 1997;16:270-6.

83. Halbert CL, Allen JM, Miller AD. Adeno-associated virus type 6 (AAV6) vectors mediate efficient transduction of airway epithelial cells in mouse lungs compared to that of AAV2 vectors. J Virol 2001;75:6615-24.

84. Ellis BL, Hirsch ML, Barker JC, Connelly JP, Steininger RJ, 3rd, Porteus MH. A survey of ex vivo/in vitro transduction efficiency of mammalian primary cells and cell lines with Nine natural adeno-associated virus (AAV1-9) and one engineered adeno-associated virus serotype. Virol J 2013;10:74.

85. Ling C, Bhukhai K, Yin Z, Tan M, Yoder MC, Leboulch P, Payen E, Srivastava A. High-Efficiency Transduction of Primary Human Hematopoietic Stem/Progenitor Cells by AAV6 Vectors: Strategies for Overcoming Donor-Variation and Implications in Genome Editing. Sci Rep 2016;6:35495.

86. Wang J, Exline CM, DeClercq JJ, Llewellyn GN, Hayward SB, Li PW, Shivak DA, Surosky RT, Gregory PD, Holmes MC, Cannon PM. Homology-driven genome editing in hematopoietic stem and progenitor cells using ZFN mRNA and AAV6 donors. Nat Biotechnol 2015;33:1256-63.

87. De Ravin SS, Reik A, Liu PQ, Li L, Wu X, Su L, Raley C, Theobald N, Choi U, Song AH, Chan A, Pearl JR, Paschon DE, Lee J, Newcombe H, Koontz S, Sweeney C, Shivak DA, Zarember KA, Peshwa MV, Gregory PD, Urnov FD, Malech HL. Targeted gene addition in human CD34(+) hematopoietic cells for

correction of X-linked chronic granulomatous disease. Nat Biotechnol 2016;34:424-9.

88. Davies JC, Moskowitz SM, Brown C, Horsley A, Mall MA, McKone EF, Plant BJ, Prais D, Ramsey BW, Taylor-Cousar JL, Tullis E, Uluer A, McKee CM, Robertson S, Shilling RA, Simard C, Van Goor F, Waltz D, Xuan F, Young T, Rowe SM, Group VXS. VX-659-Tezacaftor-Ivacaftor in Patients with Cystic Fibrosis and One or Two Phe508del Alleles. N Engl J Med 2018;379:1599-611.

89. Zhang HX, Zhang Y, Yin H. Genome Editing with mRNA Encoding ZFN, TALEN, and Cas9. Mol Ther 2019;27:735-46.

90. Nelson CE, Hakim CH, Ousterout DG, Thakore PI, Moreb EA, Castellanos Rivera RM, Madhavan S, Pan X, Ran FA, Yan WX, Asokan A, Zhang F, Duan D, Gersbach CA. In vivo genome editing improves muscle function in a mouse model of Duchenne muscular dystrophy. Science 2016;351:403-7.

91. Donaldson SH, Bennett WD, Zeman KL, Knowles MR, Tarran R, Boucher RC. Mucus clearance and lung function in cystic fibrosis with hypertonic saline. N Engl J Med 2006;354:241-50.

92. Elkins MR, Robinson M, Rose BR, Harbour C, Moriarty CP, Marks GB, Belousova EG, Xuan W, Bye PT, National Hypertonic Saline in Cystic Fibrosis Study G. A controlled trial of long-term inhaled hypertonic saline in patients with cystic fibrosis. N Engl J Med 2006;354:229-40.

VITA

Varada Anirudhan was born in Calicut, India, to Vidya Anirudhan and Anirudhan I. V. She did her schooling in St. Michael's Academy, Chennai, India, after which she went on to pursue her undergraduate studies in Industrial Biotechnology at Anna University, Chennai. Her final semester thesis project was involved in understanding DNA repair pathways in tuberculosis-causing bacteria. She then work with a startup company called Bugworks Research Pvt. Ltd. in Bangalore, India, where she studied infectious diseases such as urinary tract infection. After that, in fall 2016, she entered the Master's in Biomedical Sciences program at GSBS, UT Health, Houston, Texas. Since then, under the guidance of Dr. Brian Davis, she has been working on her thesis project.